THE TYPE IVa PILUS MACHINE IS PRE-INSTALLED DURING CELL DIVISION

THE TYPE IVa PILUS MACHINE IS PRE-INSTALLED DURING CELL DIVISION

By TYSON CARTER, B.Sc.

A Thesis Submitted to the School of Graduate Studies in Partial Fulfilment of the Requirements for the Degree Master of Science

McMaster University: Hamilton, Ontario (2016)

MASTER OF SCIENCE: Department of Biochemistry and Biomedical Science

TITLE: The type IVa pilus is pre-installed during cell division

AUTHOR: Tyson Carter B.Sc. (University of Dubuque)

SUPERVISOR: Dr. L. L. Burrows

NUMBER OF PAGES: Vii, 46

Abstract:

Type IV pili (T4P) are protein filaments found on the surface of a variety of bacterial species and mediate biofilm formation, adhesion, and flagellum-independent twitching motility. The biogenesis of T4P is dependent on a cell envelope-spanning, multiprotein complex that localizes to the poles in rod-shaped cells. How these proteins localize and cross the peptidoglycan (PG) layer in the absence of dedicated PG-hydrolyzing enzymes is unknown. In *P. aeruginosa*, PilMNOP interact to form the alignment subcomplex, connected via PilP to PilQ, which forms the outer membrane secretin. We hypothesized that polar localization and integration of the T4P machinery was driven by ordered recruitment to future sites of cell division, placing assembly system components at division septa in the correct position before daughter-cell separation. To determine which T4P components are essential for localization of the complex, we fused the T4P inner membrane assembly protein PilO to the fluorescent protein mCherry to monitor its localization. mCherry-PilO localized to the cell poles and midcell in wild type bacteria. However, it was delocalized in a strain lacking PilQ. A PilQ-mCherry fusion localized to the cell poles, likely through its putative septal PG binding AmiN domains [1,2], suggesting that PilQ binds PG and thus localizes its partners to future sites of cell division. In the absence of the associated pilotin protein (PilF), which is required for PilQ multimerization in the OM, T4P components were polarly localized, implying that localization is not dependent on secretin formation. The results of this research support a pre-installation mechanism for integration of protein complexes in the gram negative cell envelope without PG hydrolysis, which may be applicable to other systems.

Acknowledgements:

I would like to thank my supervisor, Dr. Lori Burrows, for providing me with this excellent project. Her encouragement and criticisms have been incredibly helpful throughout the course of this degree.

I would also like to thank my committee members Dr. Ray Truant and Dr. Marie Elliot. Your constructive comments helped shaped this story and allowed me to improve as a scientist.

I would like to thank Ryan Buensuceso for his invaluable tutelage on the microscope and also thank all Burrows lab members, the past two years have been great.

Lastly, I would like to thank my family for all of their support.

Table of Contents:

Section 1 - INTRODUCTION

1.1 *Pseudomonas aeruginosa* and Type IVa pili

Pseudomonas aeruginosa is a common Gram-negative bacterium that proliferates in many environmental niches. It is an opportunistic pathogen of patients with burn wounds, cystic fibrosis, and can cause corneal destruction in patients when it colonizes contact lenses [3]. While this organism has a variety of virulence factors that improve its fitness in an immunocompromised host, one that is shared by a wide range of species is the Type IV pilus (T4P).

T4P are multifunctional, fibrous appendages that protrude from the poles of rod-shaped cells [4]. They are required for adherence to both biotic and abiotic surfaces [5,6], for DNA uptake from the environment, and initiation of biofilms on surfaces [7,8]. Another function of T4P is a flagellum-independent form of motility called twitching motility. This provides the bacterium the ability to move across solid surfaces in a coordinated, social manner [9-11]. The variety of functions facilitated by T4P make them a potential target for antivirulence strategies.

1.2 Components of the T4P machinery

The T4P system is composed of four subcomplexes that together span the entire cell envelope. They include the inner membrane motor and alignment subcomplexes that form the assembly platform; the outer membrane secretin and its lipoprotein pilotin that

allows for pilus extrusion; and the pilus itself, which is dynamically assembled and disassembled by the other subcomplexes.

The pilus is composed of the major and minor pilins. The major pilin (PilA) has a highly conserved N-terminal hydrophobic alpha helix followed by a more variable hydrophilic C-terminal beta sheet domain [12]. The N-terminal helices of pilins are embedded in the inner membrane, and upon assembly, form the central core of the pilus fiber with the C-terminal domains decorating the pilus exterior [13]. The minor pilins, named for their low abundance, have a structure similar to PilA and include PilVWXE and FimU. It is proposed that the minor pilins prime assembly and are thus incorporated into the pilus fiber, potentially comprising its tip [14,15]. Both major and minor pilins are translated as pre-pilins that require processing of their short signal sequences by PilD, the prepilin peptidase, prior to assembly into the pilus fiber [16,17].

The motor subcomplex contains the inner membrane platform protein PilC and three cytoplasmic hexameric ATPases: PilB, PilT and PilU. PilB is the assembly ATPase, while PilT is the retraction ATPase. *pilB* and *pilT* mutants lack surface pili or are hyperpiliated, respectively, and both proteins show bipolar localization, while the third, PilU, is unipolar. ATPase activity and phenotypic assays of PilU variants with mutations in the Walker A (WA) and Walker B (WB) motifs confirmed that PilU has ATPase activity that is required for motility [18]. Mutants lacking PilU have surface pili that retract, because they are susceptible to killing by pilus-specific bacteriophages, but are unable to twitch [19]. PilU may control which pole is used for motility and in its absence, retraction may occur at both poles simultaneously, resulting in zero net motility [11]. Interestingly, PilT containing point

mutations in the Walker A motif failed to localize to the poles of the cell [20]. Polar localization was re-established when the mutant PilT fusion was introduced into a wild type strain, likely due to formation of mixed hexamers with wild type PilT. These data suggest that ATP binding controls oligomerization, which in turn, modulates localization.

The final component of the motor sub-complex is the platform protein, PilC. PilC has two cytoplasmic domains, each with six predicted α-helices, connected by three transmembrane segments [21]. It is thought to transduce the energy generated by the ATPases PilB and PilT to either insert pilins from the inner membrane into a growing pilus fiber, or extract them from the fiber back into the membrane, respectively [22]. While the exact arrangement of domains is still unknown in *P. aeruginosa*, the N-terminal cytoplasmic domain of PilC interacts directly with PilB and it is speculated that the C-terminal domain is required for interaction with PilT [23].

The outer membrane subcomplex is composed of PilQ and PilF. PilQ is a 12- to 14-subunit gated channel required for the translocation of the pilus fiber through the periplasm, peptidoglycan, and outer membrane [24]. PilQ has five subdomains, two N-terminal peptidoglycan-binding AmiN domains, N0 and N1 domains and the membrane-embedded secretin domain. The AmiN domains are dispensable for PilQ multimerization but required for function [24]. PilF is an outer membrane lipoprotein with six tetratricopeptide repeat (TPR) motifs, and is proposed to help shuttle PilQ monomers from the inner membrane to the outer membrane where they oligomerize [24]. Only the first four TPR motifs of PilF are essential for PilQ multimerization and there is a hydrophobic groove in the first TPR that is the likely site for a PilQ/PilF interface. The PilF interaction interface on PilQ has

yet to be identified [24]. These two proteins are essential for twitching motility in *P. aeruginosa*, as without them, the pilus is unable to cross the outer membrane.

The final subcomplex of the T4P system is the alignment subcomplex, composed of PilMNOP and possibly FimV. This complex bridges the outer and inner membrane/cytoplasmic portions of the T4P system. The cytoplasmic component, PilM, is an actin-like protein with structural similarity to cytoskeletal protein MreB and cell division protein FtsA [25,26]. PilM binds with high affinity to the short cytoplasmic N-terminus of inner membrane protein, PilN [27]. PilN interacts with inner membrane protein PilO, while PilO can also interact with itself, forming both N-O heterodimers and O-O homodimers [28]. PilN and PilO form a heterotrimer with the inner membrane lipoprotein, PilP [29]. The lipidation site at the N-terminus of PilP is dispensable for function, although its unstructured N-terminus is required for interactions with PilO and PilN [29]. Pull-down assays show that the C-terminal β-domain of PilP interacts with the N0 domain of PilQ monomers, connecting the inner and outer membrane components of the assembly system [27]. The final proposed member of the alignment sub-complex is FimV, a large, multidomain inner membrane protein with a single transmembrane segment. FimV interacts with peptidoglycan (PG) via its LysM motif, and potentially with the PilMNOP complex via its coiled-coil motif (a protein-protein interaction domain) and is required for normal secretin formation [30].

1.3 Integration of multicomponent systems through the Gram-negative cell envelope

How large multicomponent systems such as the T4P traverse the cell envelope, particularly the peptidoglycan (PG) layer, is not well understood. The average PG pore size

in a study on *E. coli* was calculated to be approximately 2-3 nm in radius, capable of allowing proteins ranging in size from 25 to 50 kDa passage through PG [31]. Many multicomponent complexes found in the cell envelope, including the T4P machinery, exceed this size. Therefore, the simplest method to integrate multi-protein systems through the cell envelope when PG pore sizes are too small is to create larger pores from existing ones to accommodate these larger proteins, which we refer to as 'retrofit' integration. Type III secretion system (T3SS) and Type IV secretion systems (T4SS) use dedicated lytic transglycosylases (LTs) to cleave glycosydic bonds within PG, creating large pores for complex integration [32,33]. Compartmentalization is also an important aspect of integration, for instance in the case of bacterial flagella. In *P. aeruginosa*, the flagellar machinery must be targeted to the cell pole before integration of the complex is complete [34]. In that system, FlgJ, the PG-hydrolyzing component of the system acts to first recognize and bind polar PG, and then to remodel the network to allow integration. However, remodelling is not an option for systems that do not have an affiliated PG-hydrolyzing component. This is apparent in the case of the Type VI secretion system (T6SS), which to date does not appear to employ dedicated PG-hydrolases for integration. This is interesting because biogenesis of T6SS complexes is not initiated until contact with a neighbouring bacterial cell [35]. This implies that the system has some method of quickly integrating through the PG barrier potentially without any PG hydrolysis. Almost all species encoding a T6SS possess either an integral T6SS component or associated component that can bind PG [36]. Therefore, PG binding may be the only essential step in cell envelope integration.

The T4P system lacks associated PG-hydrolyzing enzymes but is localized to the poles of rod shaped cells [4]. The mechanism of cell envelope integration for such systems has not yet been established. Here we show that components of the secretin and alignment subcomplexes are recruited to sites of future cell division by at least three factors, including secretin monomers that bind septal PG via their N-terminal AmiN domains. This recruitment mechanism obviates the need for PG lytic enzymes. Our data support a pre-installation, rather than retrofit, mechanism for cell envelope integration of the T4P machinery.

Section 2. MATERIALS AND METHODS

2.1 Strains, media and growth conditions

Bacterial strains, plasmids, and primers used in this study are listed in Tables 1 and 2. *Escherichia coli* and *Pseudomonas aeruginosa* were grown at 37°C in either liquid LB Lennox broth or on LB 1.5% agar plates supplemented with antibiotics. The antibiotics and their respective concentrations are as follows: ampicillin (Ap), 100 µg/ml; carbenicillin (Cb), 200 µg/ml; gentamicin (Gm), 15 µg/ml for *E. coli* strain and 30 µg/ml for *P. aeruginosa* strains, unless otherwise stated. Plasmids were transformed by heat shock into chemically competent *E. coli* cells or by electroporation into washed *P. aeruginosa* cells. All constructs were verified by DNA sequencing before use (MOBIX-McMaster University).

2.2 Plasmid transformations

Electroporation was used to introduce plasmids into *P. aeruginosa* [37]. *P. aeruginosa* cells grown overnight on solid LB-agar media with the appropriate antibiotics were scraped up and resuspended in 1 mL of nuclease free water. These resuspended cells were pelleted for 1 min at 2292 x *g* in a microcentrifuge, and then resuspended in 1 mL of nuclease free water two more times to complete the wash. After washing, 100 µl of resuspended cells in nuclease free water were pipetted into an electroporation cuvette along with approximately 250 ng of plasmid DNA. The cells were electroporated at 2.5 kV with time constants above 4 ms. Next, 900 µl of LB was added to the 100 µl of electroporated cells and left shaking at 37°C for approximately 3 hours and then plated on LB agar plates with appropriate antibiotics.

Transformation into chemically competent *E. coli* cells was achieved through heat shock [38]. $CaCl_2$ competent cells (Invitrogen) were thawed on ice and then incubated with approximately 250 ng of plasmid DNA for 30 min. Cells were then placed into a 42°C water bath for 42 s, immediately followed by incubation on ice for 2 min. These cells were resuspended in 1 mL of LB for approximately 3 h shaking at 37°C, and then plated on LB agar plates with appropriate antibiotics.

2.3 Generation of *minC* and *pilF* deletion mutants

Mutant strains were made using previously described methods [39]. Deletion constructs for generation of *minC* and *pilF* mutants were designed to include 500 nucleotides up and downstream of the gene locus to be deleted, as well as the first and last 50 nucleotides in the gene, and synthesized and cloned into pUC57 by Genscript

(Piscataway, NJ). Deletion constructs in pUC57 were sub-cloned into the pEX18Gm suicide vector [39] using the 5' BamHI and the 3' HindIII restriction sites. Once cloned into pEX18Gm, constructs were verified using DNA sequencing. After verification, the suicide vectors containing the target mutant genes (*pilF* or *minC*) were transformed into chemically competent *E. coli* SM10 cells using heat shock. The plasmids were then transferred by conjugation in a 1:9 ratio of *P. aeruginosa* to *E. coli* [39]. The mixed culture was pelleted for 1 min at 2292 x *g* in a microcentrifuge, and the pellet was resuspended in a 100 µl aliquot of LB which was spot-plated on LB agar, and incubated overnight at 37°C. Following mating, the mixed culture of cells were scraped off the LB-agar plate using a toothpick, resuspended in 1 mL of LB and the *E. coli* SM10 donor was counterselected by plating the mixture on *Pseudomonas* isolation agar (PIA; Difco) containing Gm (100 µg/ml). Gm-resistant *P. aeruginosa* colonies were streaked on LB no salt plates with sucrose (1% (w/v) bacto-tryptone, 5% (w/v) sucrose, 1.5% agar, 0.5% (w/v) bacto-yeast extract) and incubated for 16 h at 30°C. Select colonies were cultured in parallel on LB-agar and LB-agar with Gm. Gm-sensitive colonies were screened by PCR using the designated primers (Table 2) to confirm integration. Amplicons from colonies with the desired PCR profile were sequenced to confirm correct incorporation of the mutation, and the *pilF* mutant was analyzed by Western blot analysis using an α-PilF antibody at the dilution specified in Table 3 to verify loss of the gene product.

2.4 Generation of an FRT-disrupted *pilQ* mutant

A *pilQ* KO construct containing an FRT-flanked Gm cassette was previously designed [24]. This was integrated into the PAK chromosome using a Flp-FRT recombination system [39]. The suicide vector containing the disrupted *pilQ* construct (pEX18Ap::pilQ::FRTGmFRT) was introduced into chemically competent *E. coli* SM10 cells. The construct was then transferred to PAK cells through conjugation, and the SM10 cells counter-selected by plating on PIA (Pseudomonas isolation agar) media containing Gm (100 µg/ml). Gm resistant colonies were streaked onto LB no salt plates with sucrose and then incubated for 16 h at 30°C. Selected colonies were cultured in parallel on LB agar, LB agar with Gm or LB agar plus Cb. Colonies of cells that had recombined *pilQ*::FRTGmFRT onto the chromosome and excluded pEX18Ap (Cb sensitive colonies) were selected. From these colonies, the integrated Gm cassette was removed by Flp recombinase-catalyzed excision, by conjugally-transferring the Flp-expressing pFLP2 from SM10 cells into PAK cells carrying the Gm-disrupted *pilQ* gene. SM10 cells were counterselected on PIA media containing Cb (200 µg/ml). pFLP2 was removed by streaking Cb-resistant colonies on LB no salt plates containing 5% (w/v) sucrose, incubating for 16 h at 30°C. Select colonies were cultured in parallel on LB agar and LB-agar containing Gm or Cb. Cb and Gm sensitive colonies were screened by PCR using the PilQ FRT-Chk primers listed in Table 2 to confirm the retention of the FRT scar. These mutant strains were sequenced to confirm correct incorporation of the mutation, and analyzed by Western blot analysis to confirm loss of the gene product.

2.5 Generation of a mCherry-PilO fusion on the chromosome

A construct encoding an N-terminal fusion of mCherry [40] to PilO was synthesized via Genscript in the pUC57 vector. The mCherry-PilO-encoding insert was subcloned into the suicide vector pEX18Gm using the 5' EcoRI and the 3' HindIII restriction sites and constructs were verified using DNA sequencing. After verification, the suicide vector containing the fluorescent gene fusion (*mCherry-pilO*) was introduced into *E. coli* SM10 cells. The plasmid was then transferred by conjugation in a 1:9 ratio of *P. aeruginosa* to *E. coli* [39]. The mixed culture was pelleted for 1 min at 2292 x *g* in a microcentrifuge, and the pellet was resuspended in a 100 µl aliquot of LB which was spot-plated on LB agar, and incubated overnight at 37°C. Following mating, individual colonies were picked using a sterile toothpick, resuspended in 1 mL of LB and the *E. coli* SM10 donor was counterselected by plating the mixture on *Pseudomonas* isolation agar (PIA; Difco) containing Gm (100 µg/ml). Gm-resistant *P. aeruginosa* colonies were streaked on LB no salt plates with sucrose (1% w/v/ bacto-tryptone, 5% w/v sucrose, 1.5% agar, 0.5% w/v bacto-yeast extract) and incubated for 16 h at 30°C. Select colonies were cultured in parallel on LB-agar and LB-agar with Gm. Gm-sensitive colonies were screened by PCR using the designated primers found in Table 2 to confirm integration. The mCherry-PilO expressing strains were later sequenced to confirm correct incorporation of the fusion, as well as analyzed using Western blot analysis and twitching assays to verify expression of the fluorescent fusion and function of the T4P machinery, respectively.

2.6 Generation of a *pocA* deletion mutant

The *pocA* deletion construct was previously designed by the Gitai lab in the

pEX18Tc suicide vector [41]. The *pocA* deletion insert was ligated into pEX18Gm using

EcoRI and XbaI and constructs were verified using DNA sequencing. After verification, the

suicide vector containing the *pocA* deletion construct heat shocked into *E. coli* SM10 cells

and the mutant generated as described above.

2.7 Generation of a PilQ-mCherry complementation construct

An internal fusion of mCherry [40] into PilQ (between residues 132 and 133) was

synthesized via Genscript in the pUC57 vector. The PilQ-mCherry encoding insert was

subcloned into the complementation vector pBADGr [42] using the 5' EcoRI and the 3' HindIII

restriction sites and verified using DNA sequencing. The construct was then introduced into

PAK *pilQ*::FRT cells by electroporation. Expression of the PilQ-mCherry fusion was verified

using Western blot analysis with α-PilQ and α-mCherry antibodies and function was

verified using twitching assays [43].

2.8 Generation of a FimV-YFP complementation construct

The *yfp* gene encoding yellow fluorescent protein was cloned into the HindIII

restriction site in pBADGr [42]. The pBADGr mcs Fwd/Rev primers were used to confirm

correct orientation of the gene (reading 5' to 3') at this site with DNA sequencing. Next,

fimV was amplified using the FimV Clone Fwd/Rev primers listed in Table 2 and cloned into

the multiple cloning site of pBADGr upstream of the *yfp* gene by double digesting both the

vector and insert with KpnI and XbaI restriction enzymes and ligating with T4 DNA ligase as previously described [42]. Successful ligation of the insert was confirmed using the pBADGr multiple cloning site flanking primers and DNA sequencing. The construct was then electroporated into *ΔfimV* and *ΔpocA* cells. A stable fusion of YFP to the C-terminal end of FimV was confirmed using Western blot analysis with α-GFP and α-FimV antibodies. Function of the complementation construct was tested by reintroducing the vector into a *fimV* mutant, however, because twitching motility in a *fimV* mutant was not re-established this construct is non-functional.

2.9 Generation of a PilQΔAmiN complementation construct

A truncated version of PilQ lacking its AmiN domains was previously designed in the PAO1 strain [24]. We used the same boundaries to construct a truncated version of PilQ from the PAK strain. The PilQ Clone Fwd and PilQ 5' Rev primers were used to amplify the 5' end of the gene, excluding the first AmiN domain, and the PilQ N0 Fwd and PilQ Clone Rev primers were used to amplify the remainder of the gene beginning at the N0 domain and excluding the second AmiN domain (primer sequences found in Table 2). Once the amplicons were PCR purified, they were digested with XbaI in preparation for ligation using T4 DNA Ligase as previously described [42]. The ligated gene product and pBADGr were then digested with EcoRI and HindIII and ligated following the same protocol. This construct was then transformed into *E. coli* DH5α. This construct was confirmed by sequencing using the pBADGr mcs Fwd and Rev primers found in Table 2.

2.10 Generation of complementation constructs

The *pilQ, pocA* and *pilF* genes were amplified by PCR using PAK chromosomal DNA as the template (cloning primers listed in Table 2). Following purification of the amplicon, both pBADGr [42] and the amplicon were digested with the corresponding restriction enzymes (complementation vectors with corresponding restriction enzymes listed in Table 1). The digested DNA was PCR purified, and then ligated using T4 DNA ligase as previously described [42]. These ligation mixtures were then transformed into *E. coli* DH5α cells, which were then grown up overnight on LB agar plates supplemented with the appropriate antibiotics at 37°C.

2.11 Twitching motility assays

Twitching motility assays were performed as previously described [43]. Single colonies were stab inoculated to the bottom of a 1% LB-agar plate. The plates were incubated for 24 h at 30°C. Following incubation, the agar was removed and the adherent bacteria stained with 1% (w/v) crystal violet for 30 min, followed by washing with water to remove unbound dye. Twitching zone areas were measured using Fiji software [44], and zones were photographed for future reference. All experiments were performed in triplicate with at least three independent replicates.

2.12 Preparation of whole cell lysates

Cultures were grown overnight at 37°C in LB supplemented with appropriate antibiotics to an OD_{600} of 0.6. A 1 mL aliquot of cells was collected by centrifugation at

2292 x g for 1 min in a microcentrifuge. The cell pellet was resuspended in 100 μl of SDS

sample buffer (80 mM Tris (pH 6.8), 5.3% (vol/vol) 2- mercaptoethanol, 10% (vol/vol)

glycerol, and 0.02% (wt/vol) bromophenol blue, and 2% (wt/vol) SDS) and boiled for 10

min. The whole cell lysates samples were then subjected to Western blot analysis.

2.13 Western blot analysis

Whole cell lysate samples were separated on 12.5% SDS-PAGE at 80-150V in

1X running buffer and transferred to nitrocellulose membranes for 1 h at 225 mA in 1X

transfer buffer. Membranes were blocked using 5% (w/v) low fat skim milk powder in

phosphate buffered saline solution (PBS) at pH 7.4 for 1 h at room temperature on a

shaking platform, followed by incubation with the appropriate dilute antisera (found in Table

3) for 1 h at room temperature. The membranes were washed twice in 10 mL of PBS for 5

min then incubated in either goat-anti-rabbit or goat-anti-mouse IgG-alkaline phosphatase

(dependent on which animal the primary antibody was raised in) conjugated secondary

antibody (Bio-Rad) at a dilution of 1/3000 for 1 h at room temperature. The membranes

were washed twice in PBS for 5 min, and visualized with alkaline phosphatase developing

reagent (10 mL of alkaline phosphatase buffer supplemented with 100 μl of BCIP and 100

μl of NBT for development) (Bio-Rad).

2.14 Cell preparation for transmission electron microscopy

One mL of cells grown overnight in liquid culture were pelleted at 2292 x g in a

microcentrifuge and resuspended in a 1 mL solution of 2% gluteraldehyde in 0.1M sodium

cacodylate buffer at a pH of 7.4. These cells were fixed in solution for two hours at 4°C, then washed twice with sodium cacodylate buffer (pH 7.4). Then, the samples were treated with 1% osmium tetroxide in 0.1M sodium cacodylate for one hour and stained with 2% uranyl acetate overnight. After staining, the cells were dehydrated gradually with ethanol, treated with propylene oxide, embedded in Spurr's resin, and polymerized at approximately 60°C overnight. The polymerized samples were sectioned using a Leica UCT ultramicrotome and post-stained with 2% uranyl acetate and lead citrate. The prepared specimens were examined in McMaster University's Electron Microscopy Facility using the JEOL JEM 1200 EX TEMSCAN microscope (JEOL, Peabody, MA, USA) operating at an accelerating voltage of 80kV. Images were acquired with an AMT 4-megapixel digital camera (Advanced Microscopy Techniques, Woburn, MA).

2.15 Microscopy

Strains were incubated overnight at 37°C in 5 mL of LB supplemented with the appropriate antibiotics. One mL of cells were pelleted at 2292 x g in a microcentrifuge, and resuspended in 1 mL of sterile water containing 10 µg/ml Fm1-43 Fx membrane stain (Invitrogen). The cells were mixed by gentle pipetting, to ensure immersion in the dye solution, and then pelleted at 2292 x g. The pelleted cells were then stab inoculated using a pipette tip to the coverslip-media interface at the bottom of an 8 well microscope glass-coverslip slide (Lab-Tek). The cells were then incubated for 75 min at 37°C before imaging by microscopy. In filamentation experiments, 1 mL of cells grown overnight were sub-cultured into 4 mL of LB liquid media containing 40 µg/ml of cefsulodin and incubated for 3

h at 37°C. These cells were then mounted for microscopy using the above protocol. All microscopy was conducted on an EVOS Fl-auto microscope in the McMaster Biophotonics Facility. Images were acquired using a 63x oil immersion objective using a TexasRed filter, YFP filter, or brightfield (no filter). Adjustment of image brightness and contrast as well as generation of overlaid images were performed using Fiji [44].

2.16 Quantification of mCherry-PilO fluorescence

Fiji [44] was used to quantify fluorescence. Each field of cells image in the TexasRed filter set and the YFP filter set was overlaid (Process > Image Calculator), and this combined micrograph and the micrograph in the YFP filter set were used for the remaining steps. Next, a scale was manually applied (412 pixels per 50 μm) to both the overlay and the YFP field (Analyze > Set Scale). A 250 μm^2 grid was then added to both fields to allow precise documentation of which cells were included in the quantification (Analyze > Tools > Grid > each square set to 250 μm^2). Moving systematically from each square in the grid, cells that fulfilled the following criteria were selected: 1) the cell was not in contact with other cells; 2) the cell had normal morphology (excluding minicells, cells undergoing lysis, etc.); 3) the cell must have a stable mCherry-PilO fusion (diffuse fluorescence implies cleavage of the tag in that cell). Once 50 cells had been counted using these criteria, they were each saved individually twice, once as the overlay and once in the YFP field (Box draw tool to select cell > Image > Duplicate). Once saved, the line draw tool (line width set to 10) was used on each cell in both fields to measure pixel intensity from one cell pole to the other (Trace line over cell > Command 'K' > save pixel

intensity graph as data points in excel file). Once all the cell length versus pixel intensity data was saved in an Excel spreadsheet for 50 cells, all cell lengths were normalized to 1 (divide each data point associated with length by the total length of the cell measured to yield 0-1 scale). Then we subtracted the pixel intensity measurements in the YFP field from the overlay field, producing mCherry-PilO pixel intensity measurements alone in each cell on a scale from 0 to 1. These data were transferred to the Prism Graphpad software to be represented as data plots on an XY scatter plot, to show the distribution of mCherry-PilO fluorescence versus the cell length.

Section 3 - RESULTS

3.1 mCherry-PilO localizes to cell poles and future cell division sites

To track the localization of the T4P alignment subcomplex under physiological conditions, we generated a construct encoding an in-frame fusion of mCherry to the free cytoplasmic amino terminus of the PilO protein, and integrated it at the native *pilO* locus on the *P. aeruginosa* chromosome (Fig. 1A). The fusion was stable as determined by western blot with anti-PilO antisera, and had minimal effects on twitching motility, showing that it was functional (Fig. 1B).

The fusion protein localized to both poles in all cells, as well as to the midpoint of cells undergoing division (Fig. 1C). To better visualize this localization pattern, cells were filamented using sub-MIC levels of cefsulodin to inhibit PBP3 (FtsI), a late-stage cell division transpeptidase [45], arresting dividing cells prior to invagination. mCherry-PilO localized to the poles and to regularly spaced intervals in filamented cells, suggestive of

recruitment to future sites of cell division (Fig. 1D). Fiji [44] was used to quantify localization

in n = 50 cells, showing fluorescence at the cell poles (Fig.1E).
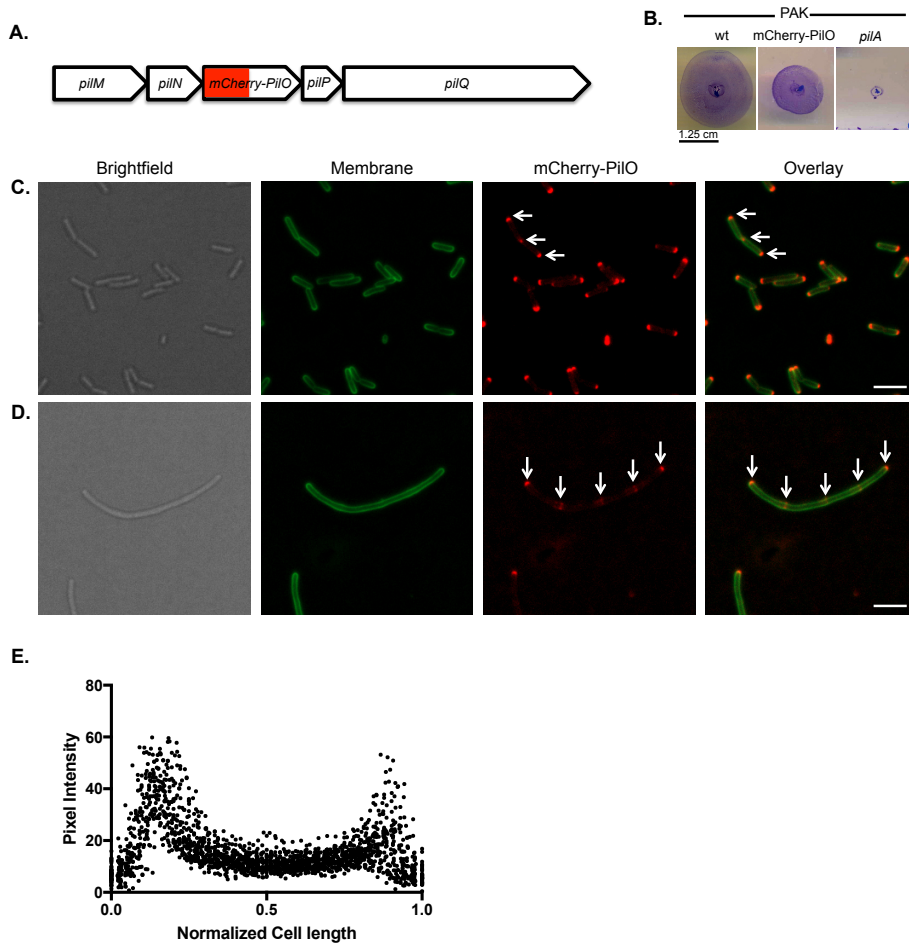

Figure 1. mCherry-PilO localizes to cell poles and also future sites of cell division in *P. aeruginosa*. A) T4P assembly complex operon map showing 5' placement of the *mCherry* gene in tandem with *pilO*. B) Twitching assay demonstrating the mCherry-PilO fusion protein's affect on twitching motility in PAK cells. C) mCherry-PilO localizes to the poles of wt cells and also the septum in late-stage dividing cells. D) When cells are filamented with 40 µg/ml cefsulodin, mCherry-PilO localizes to the poles and at regularly spaced foci (arrows). E) mCherry pixel intensity quantification from one cell pole to the other (0-1) in 50 randomly selected cells from the population. Scale Bar = 3 µm. Cell membranes are stained using FM1-43FX dye (in 10 µg/ml dye solution). Cells were stab-inoculated into 1% LBA in chambered glass coverslips, incubated at 37°C and imaged using the 63x oil immersion objective on an EVOS-FL digital imaging system. Images were processed using Fiji.

To confirm that the mCherry-PilO was recruited to sites of future cell division, we

deleted the gene encoding MinC, a key component of the oscillating Min system required

for inhibition of FtsZ polymerization at non-midcell locations [46,47]. Cells lacking MinC exhibit

aberrantly localized septa, producing mini-cells due to unequal cell division (Fig. 2A). As

predicted, the mCherry-PilO fusion localized to aberrant septal sites (Fig. 2B). Together,

these data suggest that under physiological conditions, PilO – and by inference its partners, PilMN and PilP – are recruited to future sites of cell division prior to invagination.
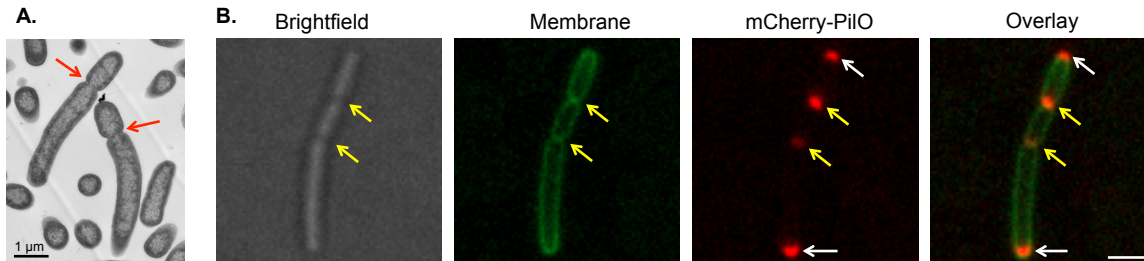

Figure 2. mCherry-PilO localizes to aberrantly localized septa in a *minC* mutant. A) MinC regulates divisome placement by inhibiting FtsZ polymerization at sites other than mid-cell. In the absence of minC, cells exhibit aberrant division sites (red arrows). B) mCherry-PilO localization is abnormal in the absence of MinC. Polar foci highlighted with white arrows and sub-polar foci highlighted with yellow arrows. Scale Bar = 1 µm. Cell membranes are stained using FM1-43FX dye (in 10 µg/ml dye solution). Cells were stab-inoculated into 1% LBA in chambered glass coverslips, incubated at 37°C and imaged using the 63x oil immersion objective on an EVOS-FL digital imaging system. Images were processed using Fiji.

3.2 T4P assembly complex proteins localize to cell poles independently of the actin-like protein, PilM

To define the mechanism of recruitment of the T4P assembly machinery to sites of future cell division, we first examined the effects of removing specific components of the alignment subcomplex. The cytoplasmic component of the assembly complex, PilM, has pronounced structural similarity to the early divisome protein, FtsA [25,26]. FtsA is a peripheral membrane protein that interacts with FtsZ, tethering it to the membrane. Based on its structural mimicry of FtsA, we hypothesized that PilM, and thus the alignment subcomplex, might be recruited to midcell by interactions with FtsZ [48]. In a *pilM* deletion background, mCherry-PilO continued to exhibit polar and midcell localization (Fig. 3AB), ruling out PilM as a driver of midcell recruitment.

3.3 The outer membrane secretin subunit and PG-binding protein, PilQ, is required for localization of T4P assembly components

The PilMNOP alignment subcomplex connects with the secretin via interactions of PilP with the N0 domain of PilQ. Preceding the N0 domain in *P. aeruginosa* PilQ are two tandem AmiN domains, which are proposed to bind septal PG [1,24,49]. Since *pilMNOPQ* are expressed from a single operon, we hypothesized that recruitment of PilMNOP to sites of future cell division might occur through a PilMNOP-PilQ-septal PG interactions. We first deleted *pilQ* in the mCherry-PilO expressing strain, and monitored localization of the fusion. In the absence of PilQ, mCherry-PilO was delocalized (Fig. 3CD). To confirm that loss of mCherry-PilO localization in the *pilQ* strain was due to loss of PilP-PilQ interactions, we next deleted *pilP* in the mCherry-PilO strain. In this background, mCherry-PilO was also delocalized (Fig. 3EF), supporting the hypothesis that recruitment of PilQ to midcell is the primary event, and the remaining assembly subcomplex components are recruited via PilP's interaction with PilQ.

To test whether its tandem AmiN PG-binding domains were responsible for localization of PilQ and its partners to midcell, we complemented *pilQ* cells expressing mCherry-PilO with full length PilQ, or an N0-N1 and secretin domain construct missing both AmiN domains, which was previously shown to form stable but non-functional secretin oligomers [24]. Full length PilQ restored the wild type pattern of mCherry-PilO localization in a *pilQ* mutant (Fig. 4CD), while the fusion remained delocalized when AmiN-less PilQ was provided (Fig. 4EF). These data suggested that localization of T4P assembly components was dependent upon PilQ's AmiN domains that confer the ability to interact with PG.
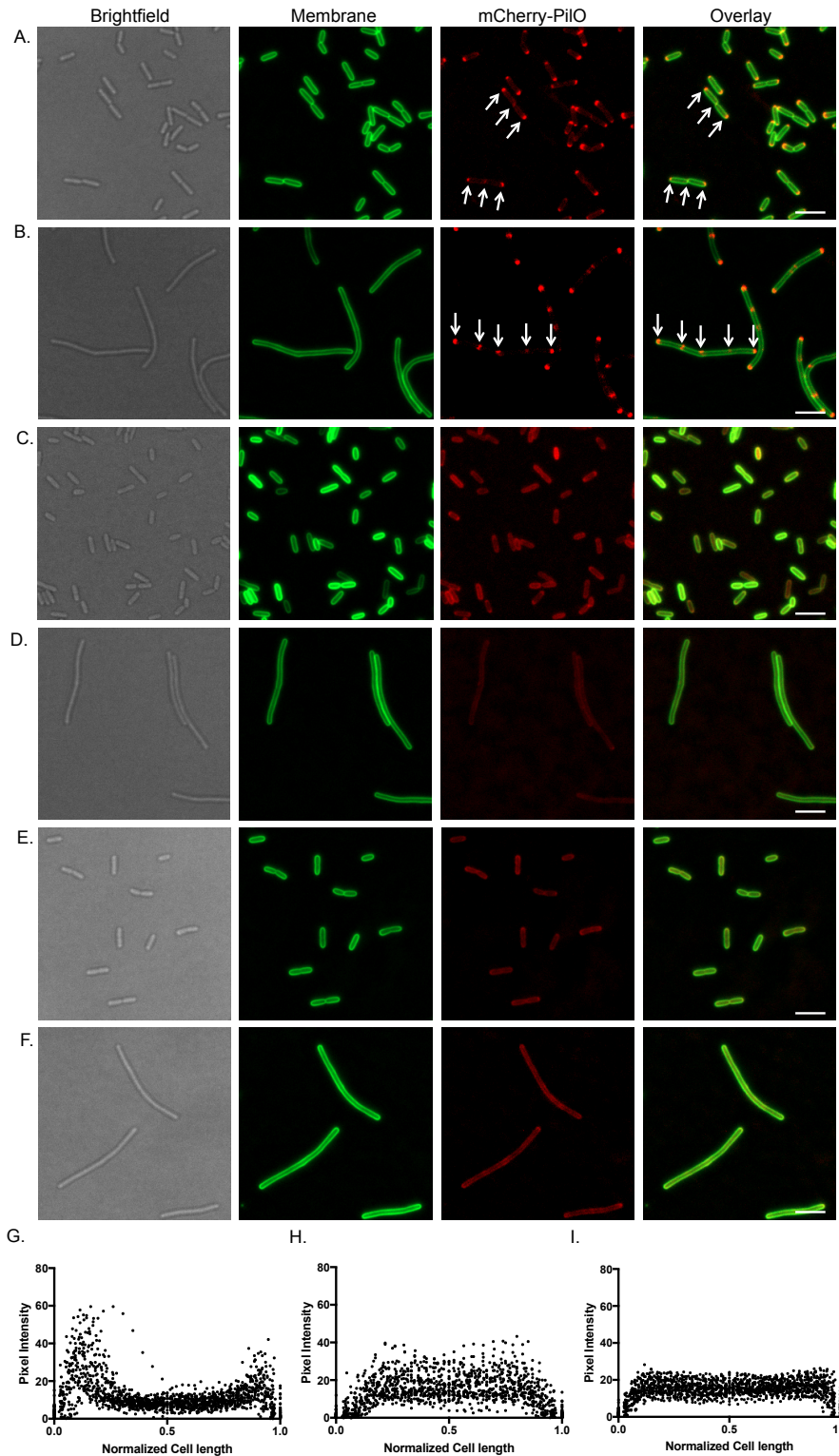
Figure 3. T4P assembly complex localization is dependent on the outermost components rather than the innermost components. A-B) mCherry-PilO retains polar and septal localization, as well as polar and regularly spaced foci localization when treated with 40 µg/ml cefsulodin , in the absence of PilM. C-D) In the absence of PilQ, both untreated and antibiotic-treated cells exhibit mislocalized mCherry-PilO throughout the cell membrane. E-F) In the absence of PilP, the periplasmic assembly complex linker protein, mCherry-PilO is mislocalized in both untreated and antibiotic-treated cells. G-I) mCherry pixel intensity quantification from one cell pole to the other (0-1) in 50 randomly selected cells from the population in the absence of *pilM* (G), *pilQ* (H), and *pilP* (I). Scale Bar = 3 µm. Cell membranes are stained using FM1-43FX dye (in 10 µg/ml dye solution). Cells were stab-inoculated into 1% LBA in chambered glass coverslips, incubated at 37°C and imaged using the 63x oil immersion objective on an EVOS-FL digital imaging system. Images were processed using Fiji.

Figure 4. Reintroduction of a truncated version of PilQ lacking its PG-binding (AmiN) domains does not re-establish proper localization of mCherry-PilO. A) Domain map of full length PilQ, PG-binding domains shown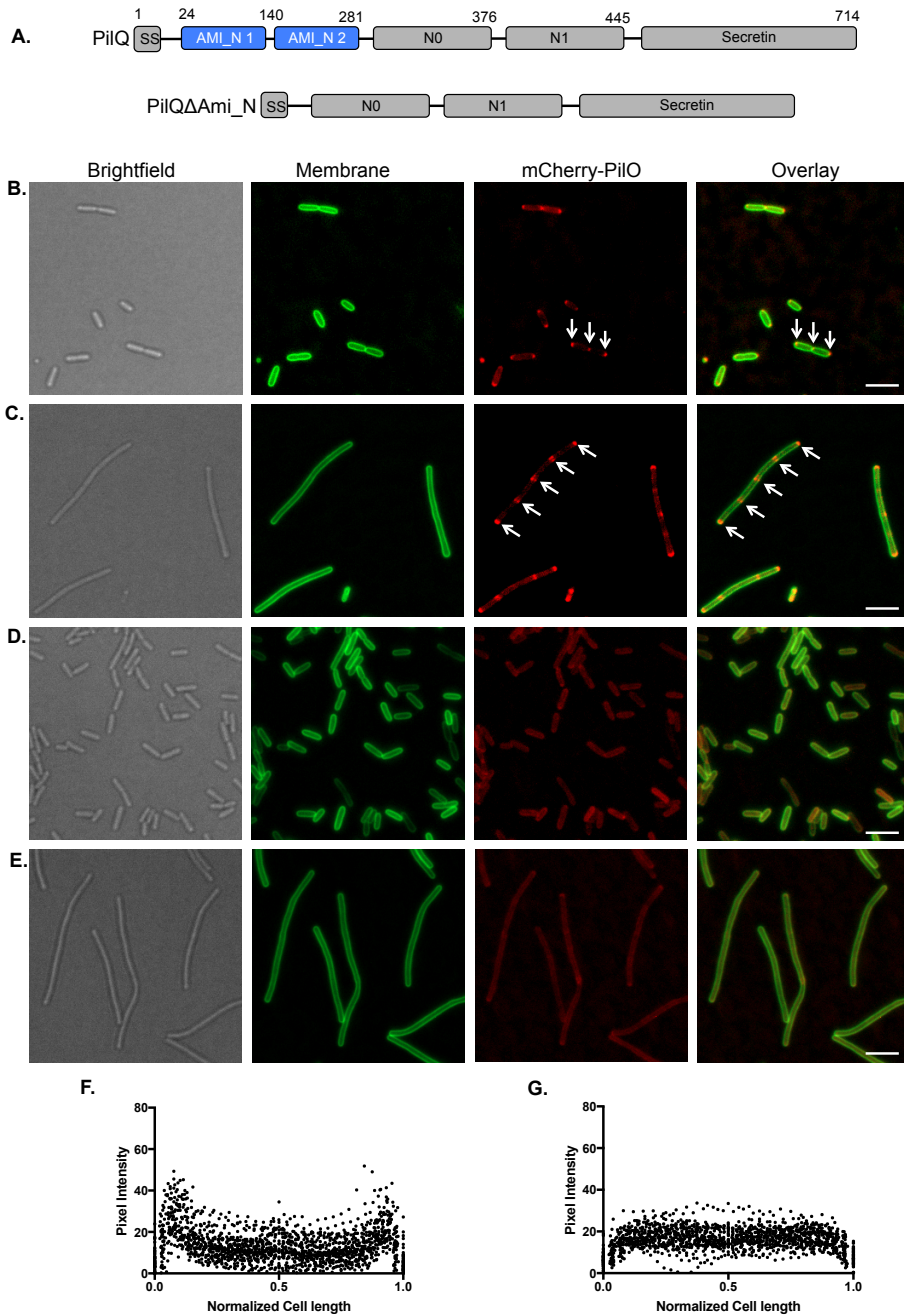 in blue. B) Domain map of truncated-PilQ. C-D) Reintroduction of full length PilQ *in trans* into cells lacking *pilQ* re-establishes polar and septal localization (white arrows) of mCherry-PilO in untreated cells, and also polar and regularly spaced foci localization in cells treated with 40 µg/ml cefsulodin. E-F) When the truncated version of PilQ is reintroduced *in trans* into cells lacking *pilQ*, mCherry-PilO is mislocalized throughout the cell membrane in both untreated and antibiotic-treated cells. G-H) mCherry pixel intensity quantification from one cell pole to the other (0-1) in 50 randomly selected cells from the population in cells expressing either full length PilQ (G) or cells expressing truncated-PilQ (H). Scale Bar = 3 µm. Cell membranes are stained using FM1-43FX dye (in 10 µg/ml dye solution). Cells were stab-inoculated into 1% LBA in chambered glass coverslips, incubated at 37°C and imaged using the 63x oil immersion objective on an EVOS-FL digital imaging system. Images were processed using Fiji.

3.4 Localization of mCherry-PilO precedes PilQ oligomerization

The *Myxococcus xanthus* T4P system – which is similar to that of *P. aeruginosa* – was proposed to assemble in an 'outside-in' manner, with the PilMNOP alignment subcomplex interacting with the PilQ secretin complex after it assembles in the outer

22
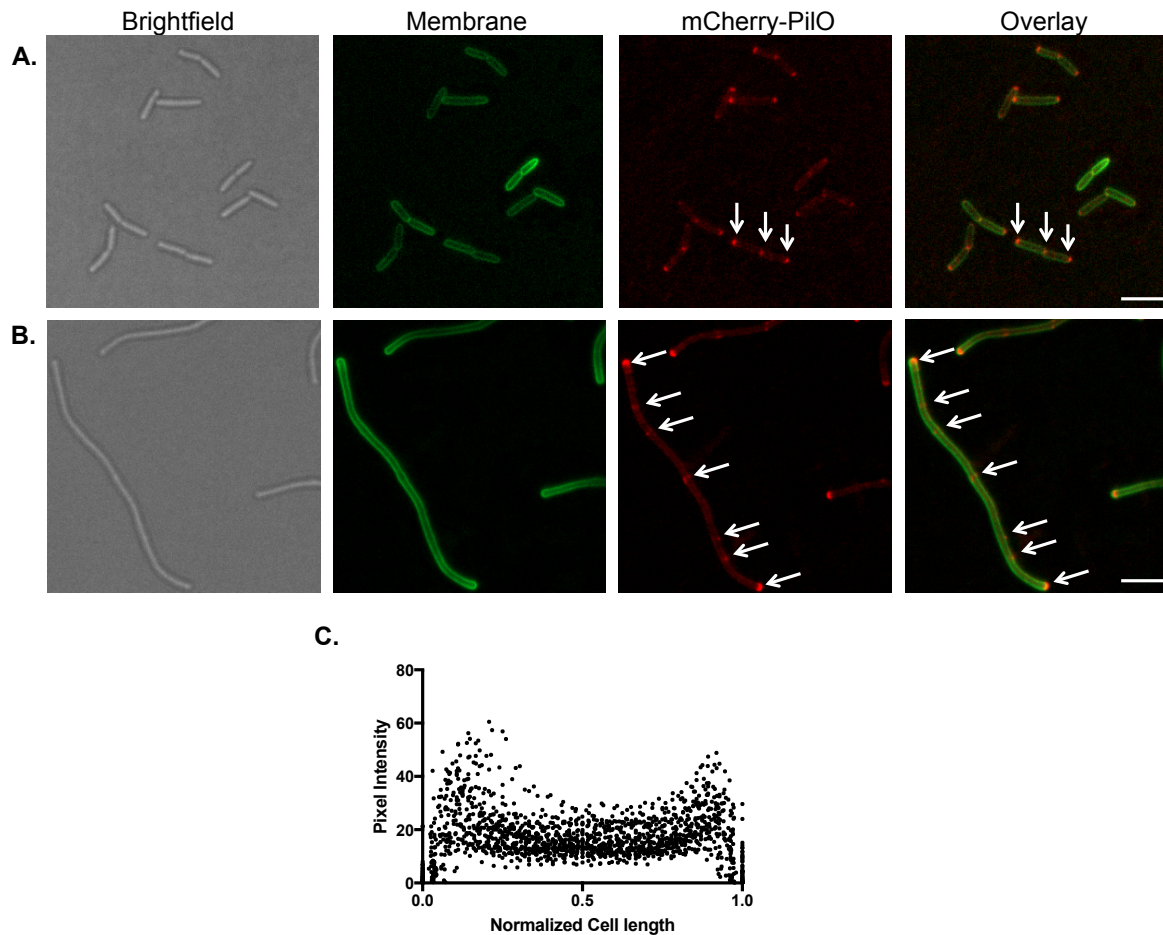
Figure 5. In the absence of the dedicated pilotin protein, PilF, PilQ monomers are still capable of recruiting the T4P assembly complex to the cell poles and septum. A) mCherry-PilO localizes to the poles and septa of late-stage dividing cells, marked by white arrows. B) When cells are filamented with 40 μg/ml cefsulodin, mCherry-PilO localizes to the poles and regularly spaced foci (arrows). C) mCherry pixel intensity quantification from one cell pole to the other (0-1) in 50 randomly selected cells from the population. Scale Bar = 3 μm. Cells were stab-inoculated into 1% LBA in chambered glass coverslips, incubated at 37°C and imaged using the 63x oil immersion objective on an EVOS-FL digital imaging system. Images were processed using Fiji.

membrane [50]. However, those data were not consistent with our observation that mCherry-PilO localized to future sites of division in filamented cells, where the outer membrane is not yet present due to division arrest prior to invagination (Fig 1). To test whether secretin assembly was a necessary prerequisite in the recruitment process, we examined the localization of mCherry-PilO in mutants lacking the pilotin for PilQ, the outer membrane lipoprotein, PilF. In the absence of PilF, PilQ remains in a monomeric state in the inner

membrane [24]. In a *pilF* strain, the localization pattern of mCherry-PilO was similar to wild type (Fig. 5). These data confirm that localization of T4P components to midcell precedes multimerization of the secretin.

3.5 Additional factors modulate T4P assembly machinery localization

        FimV is a T4P-associated protein required for twitching motility and contains a highly conserved PG-binding LysM motif at its N-terminus [51]. We showed previously [30] that PilQ multimer formation is reduced in a *fimV* mutant, which made FimV of interest in this study. In the absence of FimV, PilQ-mCherry expressed in untreated cells exhibited peripheral fluorescence in the cell envelope but polar foci were detectable (Fig. S1). mCherry-PilO, however, was completely delocalized in the absence of FimV (Fig. 6AB) along with PilQ-mCherry expressed in filamented cells (Fig. S2). We previously generated a strain expressing full-length FimV with an in-frame deletion of its PG-binding LysM motif [30]. PilQ and PilO were delocalized in the ΔLysM FimV strain (Fig. 6CD, S1 and S2) in the same fashion as the *fimV* mutant, suggesting that interactions of both PilQ and FimV with PG are important first steps in the localization process.

        During a mutant screen for factors required for correct localization of *P. aeruginosa's* single polar flagellum, the Gitai lab identified a putative protein complex that they named PocAB -TonB3 for 'polar organelle coordinator' [41]. They subsequently found that all three components were also required for expression and/or polar localization of T4P. *pocA* mutants made a few, non-polar pili, while *pocB* and *tonB3* mutants failed to produce pili. The mechanism by which this system controls polar localization of motility

organelles is not yet clear, since the Poc proteins themselves were not localized to the poles [41].

We deleted *pocA* in cells expressing either PilQ-mCherry (Fig. S1, S2) or mCherry-PilO (Fig. 7AB). PilQ-mCherry was observed in untreated cells in the cell envelope although polar foci are present (Fig. S1), while in filamented cells, delocalization was more obvious (Fig. S2). mCherry-PilO became completely delocalized in the absence of *pocA*, while wild type localization of mCherry-PilO was re-established upon complementation with *pocA in trans* (Fig. 7CD). Interestingly, while both PocA and FimV are required for T4P assembly component localization, they appear to act independently of one another, as FimV remains polarly localized in a *pocA* mutant (Fig. 8).
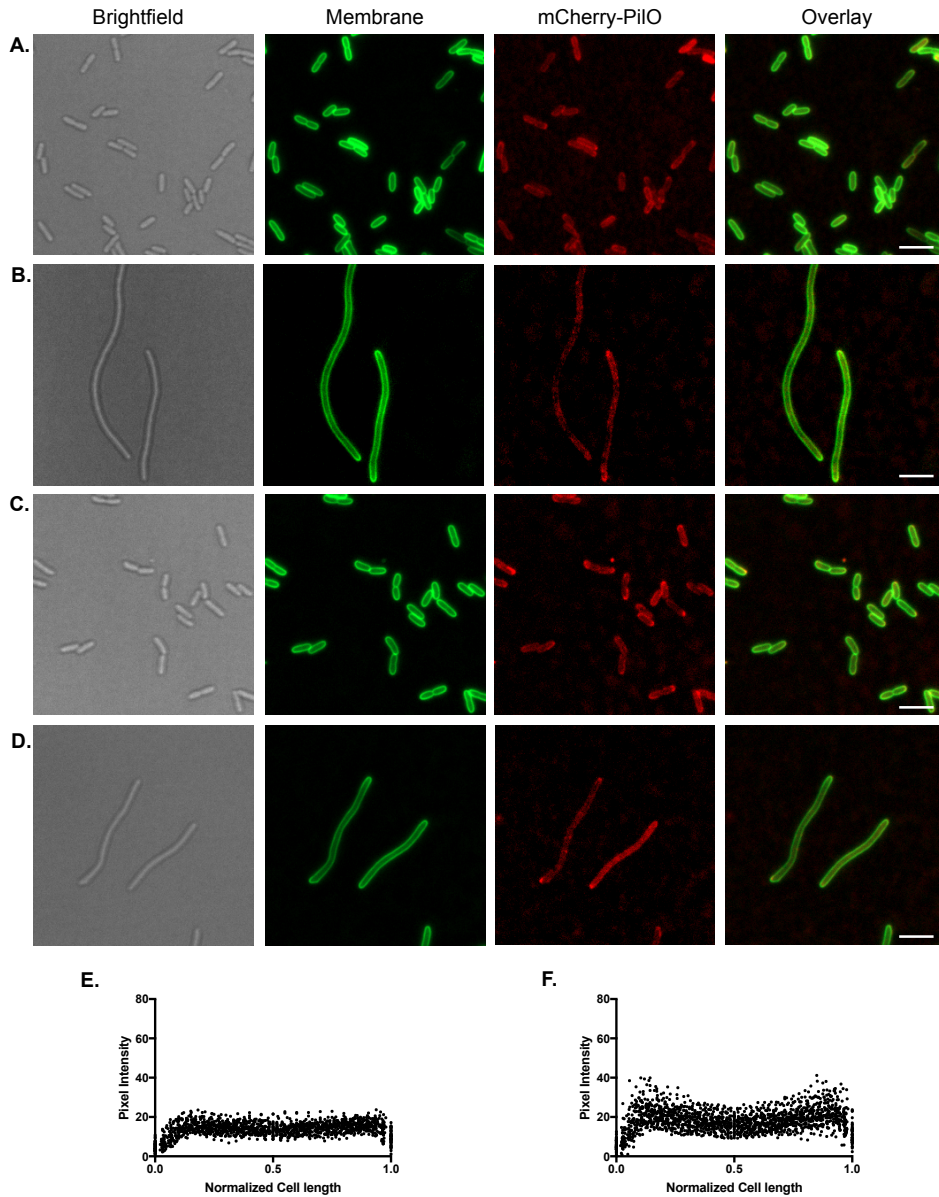
Figure 6. The multifunctional PG-binding protein FimV is essential for proper localization of T4P assembly complex components. A-B) In the absence of FimV, both untreated cells and cells treated with 40 µg/ml cefsulodin exhibit mislocalized mCherry-PilO throughout the cell membrane C-D) In cells expressing a truncated version of FimV lacking its PG-binding domain (LysM), mCherry-PilO is mislocalized throughout the cell membrane in both untreated and antibiotic-treated cells. E-F) mCherry pixel intensity quantification from one cell pole to the other (0-1) in 50 randomly selected cells from the population in cells lacking full length FimV (E) or cells expressing truncated-FimV lacking the LysM domain (F). Scale Bar = 3 µm. Cell membranes are stained using FM1-43FX dye (in 10 µg/ml dye solution). Cells were stab-inoculated into 1% LBA in chambered glass coverslips, incubated at 37°C and imaged using the 63x oil immersion objective on an EVOS-FL digital imaging system. Images were processed using Fiji.
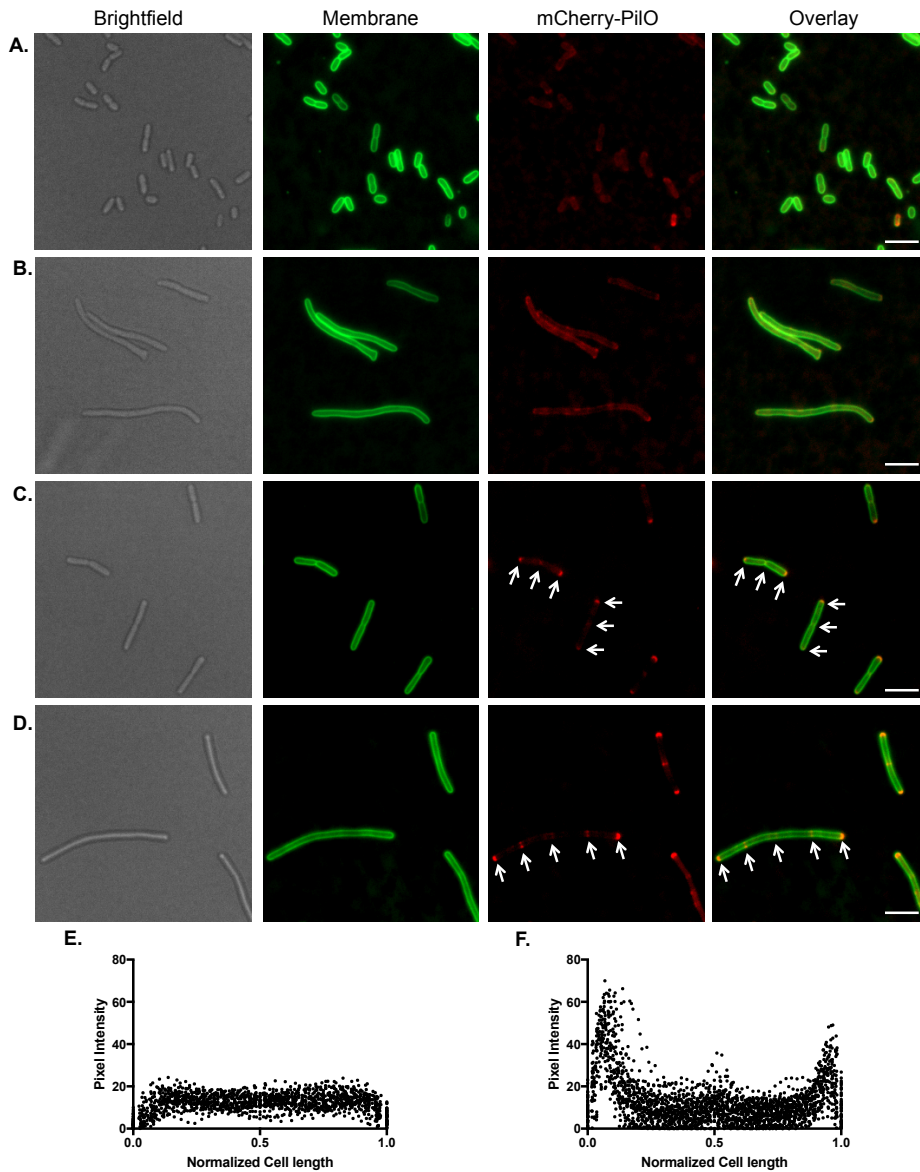
Figure 7. mCherry-PilO mislocalizes in a *pocA* mutant. A-B) In the absence of the polar organelle coordinating protein, PocA, mCherry-PilO becomes mislocalized in both untreated cells and cells treated with 40 µg/ml cefsulodin. C-D) When PocA is reintroduced *in trans*, mCherry-PilO localization to the poles and septum is recovered (white arrows) in untreated cells, as well as the poles and regularly spaced foci in antibiotic-treated cells. E-F) mCherry pixel intensity quantification from one cell pole to the other (0-1) in 50 randomly selected cells from the population in either cells lacking pocA (E) or in cells that have had pocA reintroduced (F). Scale Bar = 3 µm. Cell membranes are stained using FM1-43FX dye (in 10 µg/ml dye solution). Cells were stab-inoculated into 1% LBA in chambered glass coverslips, incubated at 37°C and imaged using the 63x oil immersion objective on an EVOS-FL digital imaging system. Images were processed using Fiji.

Brightfield	Membrane	FimV-YFP	Overlay
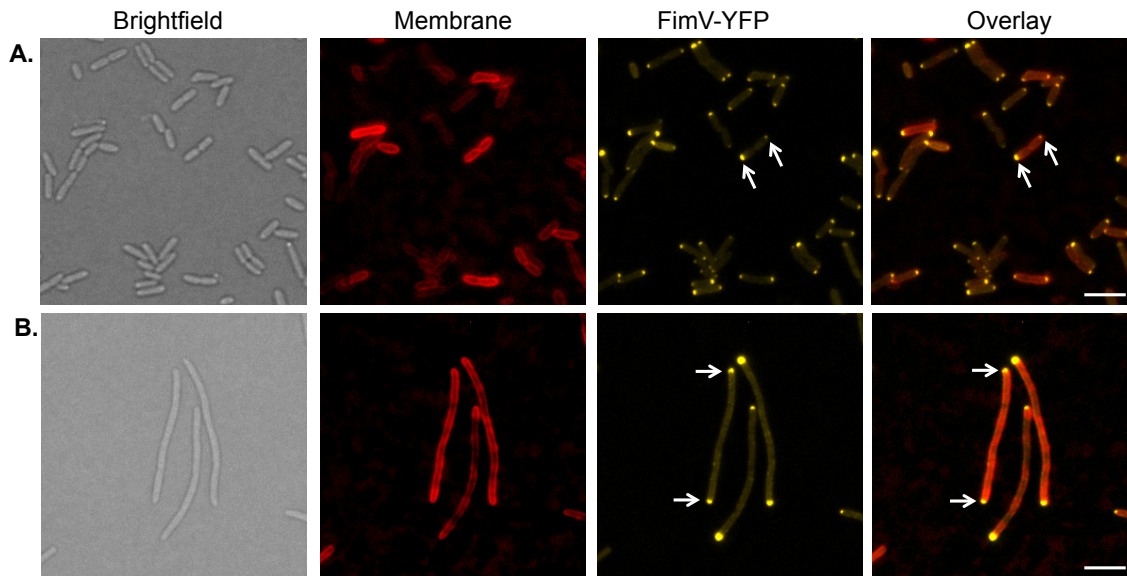
Figure 8. FimV remains polarly localized in the absence of PocA. A) FimV-YFP remains localized to the cell poles (arrows) when PocA is not expressed. B) FimV-YFP localizes to the poles in cells treated with 40 µg/ml cefsulodin. Scale Bar = 3 µm. The FimV-YFP construct's expression was induced using 0.1% arabinose via the pBADGr expression vector in *P.* aeruginosa cells. Cell membranes are stained using FM1-64FX dye (in 20 µg/ml dye solution). Cells were stab-inoculated into 1% LBA in chambered glass coverslips, incubated at 37°C and imaged using the 63x oil immersion objective on an EVOS-FL digital imaging system. Images were processed using Fiji.

Section 4 - DISCUSSION

Here we showed that components of the T4P alignment subcomplex and the secretin are recruited to sites of future cell division, and that at least three independent mechanisms participate in this process. For PilQ and FimV, recruitment depends on their ability to bind PG, as loss of the AmiN domains (PilQ) or LysM motif (FimV) results in delocalization.

Recruitment of mCherry-PilO to midcell was dependent on the secretin monomer PilQ (Fig. 3C-D), but deletion of the pilotin protein PilF had no effect (Fig. 5). Therefore, interaction of PilMNOP and PilQ and confinement at future division sites occurs prior to secretin oligomerization. Previous studies of T4P assembly system formation in *M.xanthus*

suggested that PilQ multimerization was essential for the recruitment of additional T4P assembly components, because loss of Tgl – the equivalent of PilF – abrogated polar localization of PilQ and thus, other T4P proteins. These data supported an 'outside in' model for *M. xanthus* T4P system formation which depended on PilQ oligomerization [50]. Interestingly, *M. xanthus* PilQ was suggested to localize to the septum either "late during cell division, or immediately after". These data are consistent with PilQ localization in *P. aeruginosa*, however the pilotin proteins in *M. xanthus* and *P. aeruginosa* may play different roles.

What is clear is that PilQ monomers, in both species, will localize to nascent polar sites in dividing bacteria ([50] and this work). The septum (and cell poles) are thought to contain PG that has fewer peptide side chains due to the activity of the *N*-acetylmuramyl-*L*-alanine amidases, enzymes required for septal PG splitting at the septum to allow for daughter cell separation [52-54]. This form of PG is the binding target for multiple protein motifs found in various species of bacteria [30,55-57]. Both *P. aeruginosa* and *M. xanthus* PilQ have N-terminal AmiN domains (2 per monomer in *P. aeruginosa*, and 3 per monomer in *M. xanthus*) which are also characterized as septal PG-binding motifs and speculated to be involved in anchoring multicomponent to the PG layer [1,2]. *Neisseria gonorrhoeae* and *N. meningitidis* PilQ monomers also contain two N-terminal AmiN domains [1], but due to their coccoid shapes, express peritrichous T4P. It's possible that they use a similar mechanism of T4P component recruitment to the division plane, and due to lack of lateral cell wall elongation during growth, are essentially two closely apposed, piliated poles.

Many secretion systems have well characterized methods for cell envelope integration, usually following a retro-fit model that involves expression of a dedicated PG-hydrolyzing enzyme, such as a muramidases in the case of the flagellar system, and lytic transglycosylases in Type III and IV secretion systems [32-34,58]. The T4P system appears to use a pre-installation model instead. Binding of specific components such as PilQ to PG could initiate integration in the absence of PG-hydrolyzing enzymes, and this may be a universal process. In the *Escherichia coli* Type VI secretion system (T6SS), loss of SciZ, a PG-binding factor, abolishes activity of the complex which implies that PG binding is an essential step in function and possibly integration of this system [36]. It is worth noting that many T6SS systems include a component that contains a PG-binding domain, either an OmpA-like or SPOR domain [36]. Alternatively, while the Type II Secretion system in *P. aeruginosa* may not bind PG at the poles, it was demonstrated that active secretion of effectors occurs at the poles [59], and the function of this system is dependent on the non-associated protein FimV [60]. Interestingly, we have demonstrated in this work that a loss of FimV results in mislocalization of components of the closely related T4P system (Fig. 6). Therefore, while FimV indirectly regulates T2SS expression by controlling cAMP production [61], it also has a potential stabilizing effect on the secretion system [60] one that may influence polar localization and integration as it does with the T4P. Similarly, in *Mxyococcus and Neisseria* species, an unrelated PG-binding protein called TsaP is required for T4P function [62]. Although *P. aeruginosa* has a gene encoding a putative TsaP orthologue, deletion mutants have no motility or piliation phenotypes (Koo et al., 2016, in press).

Cowles *et al* [41] reported that *P. aeruginosa* mutants lacking the polar organelle coordinating (Poc) proteins lost polar localization of both the single polar flagellum and the T4P, but they were unable to shed light on the mechanism. We showed the T4P assembly complex is delocalized in a *pocA* mutant (Fig. 7) while FimV remains bipolar (Fig. 8). The Poc protein complex itself is not localized to the poles in *P. aeruginosa* [41]. How could non-polar proteins indirectly facilitate polar recruitment of essential virulence factors? And why would the organism use multiple strategies to accomplish the same goal? Or are these processes in fact distinct?

The PocA-PocB-TonB3 protein complex is homologous to the ExbB-ExbD-TonB complex in *E. coli* [41] which energizes siderophore uptake across the outer membrane [63,64]. The PG network is constantly being remodelled by the elongosome throughout the life cycle of the cell [65], perhaps deletion of these proteins affects how the this process is energized in *P. aeruginosa*. The resulting subtle structural differences in PG architecture might affect binding of PG targeting motifs.

Together, these data allow us to propose a "pre-installation" model for T4P assembly complex integration in *P. aeruginosa*. We suggest that the T4P assembly proteins (PilMNOPQ) are co-translated into the inner membrane, where they form a subcomplex that diffuses laterally in the membrane until the AmiN domains of the PilQ monomer recognize and bind to septal PG. One "unit" of the assembly complex (monomeric-PilMNOPQ) is therefore likely bound to the septal PG network, which would conceivably have pore sizes large enough for translocation of PilQ monomers towards the OM as the cell undergoes division. The next step is unclear, because the oligomerization

pathway for PilQ in the OM has not been discovered [24]. It was demonstrated in *N. gonorrhoeae* that certain point mutations in the PilQ-secretin domain can disrupt function of the T4P to different extents [66]. This may suggest that PilQ adopts intermediate conformations as it traverses the PG layer before oligomerization in the OM. Does the pilotin aid in PilQ translocation across the periplasm? Or do PilQ monomers translocate to the OM by another means, such as protein-protein interactions observed in cell envelope spanning protein complexes present such as LpoA and PBP1a at the divisome[67]? This question remains to be answered, although we hypothesize that the integration process is one fluid step that brings one unit of the assembly complex through a PG pore for multimerization in the OM as invagination is ongoing. This model could explain how the T4P is integrated through the PG barrier in the absence of PG-remodelling enzymes, and possibly could provide insight into multi-component integration strategies in other systems.

Section 5 – CONCLUSIONS AND FUTURE DIRECTIONS

5.1 Future Directions

While we have shown how two of the three T4P machine subcomplexes localize to the cell poles in *P. aeruginosa*, we don't yet understand how the motor subcomplex including PilC, the essential platform protein [23] becomes enclosed in the cylindrical structure formed by PilMNOPQ. We showed that the soluble cytoplasmic ATPases that power the pilus machinery (PilB and PilT) localized to the cell poles as well as to midcell in dividing cells [18], although the targeting mechanism was unknown. Localization studies such as we describe here could be done to determine the dependence of PilC localization on

other T4P components.

Another aspect of the localization process that is not well understood is when/how PilQ monomers are translocated through the PG for OM insertion. It has been postulated that PilF may be involved (in concert with the Lol protein system) in translocation across the periplasm [24], however the PilF equivalent in *Myxococcus* can be shared between neighbouring bacteria and is not exclusively polar [68]. This may imply that pilotins are not universally involved in translocation of secretin subunits to the OM. Fluorescent microscopy could be used to observe the timing of PilF and PilQ translocation in tandem, which would allow us to visualize whether these both proteins translocate at the same time.

An additional uncharacterized aspect of this project is how exactly FimV is involved in the localization process. Unpublished bacterial two-hybrid data from our lab revealed that FimV interacts directly with PilO and PilS, a bipolar IM sensor kinase responsible for transcriptional regulation of PilA [69]. In its absence both proteins are delocalized. Both of these proteins are found in the IM with FimV, therefore perhaps FimV is required to recruit these IM proteins to the cell poles via interaction with PG through its LysM domain [30,55]. Continued work on FimV and its interaction partners within the T4P machinery will inevitably improve our understanding of this localization process.

5.2 Conclusions and Significance

There are many multiprotein secretion systems whose mechanisms of integration into the gram negative cell envelope remain a mystery. Many of these secretion systems are expressed in pathogens of humans, animals, and plants [70,71]. Furthering our

understanding of these processes could lead to novel methods of interfering with the localization, biogenesis, and ultimately, the function of these bacterial weapons.

We demonstrated that outer and inner membrane components (PilQ and PilO) of the T4P assembly complex are recruited to future cell division sites in dividing cells, supporting our hypothesis that they are preinstalled. The localization of the assembly complex is dependent on PilQ monomers that can bind septal PG through their AMIN domains [1,2,24]. We propose that the remaining assembly complex proteins are pulled into position in the periplasm remaining anchored in the IM, facilitated by PilQ as it translocates through PG pores for multimerization in the outer membrane [24]. Although we have shown that the recruitment of the T4P assembly complex requires PilQ interaction with PG, FimV and the Poc complex are also involved. How these other factors affect this process remains to be elucidated.

Section 6 – REFERENCES

1. Rocaboy, M. *et al.* The crystal structure of the cell division amidase AmiC reveals the fold of the AMIN domain, a new peptidoglycan binding domain. *Molecular Microbiology* **90,** 267–277 (2013).
2. de Souza, R. F., Anantharaman, V., de Souza, S. J., Aravind, L. & Gueiros-Filho, F. J. AMIN domains have a predicted role in localization of diverse periplasmic protein complexes. *Bioinformatics* **24,** 2423–2426 (2008).
3. Lyczak, J. B., Cannon, C. L. & Pier, G. B. Establishment of *Pseudomonas aeruginosa* infection: lessons from a versatile opportunist. *Microbes and Infection* **2,** 1051–1060 (2000).
4. Bradley, D. E. A function of *Pseudomonas aeruginosa* PAO polar pili: twitching motility. *Canadian Journal of Microbiology* **26,** 146–154 (1980).
5. Berne, C., Ducret, A., Brun, Y. V. & Hardy, G. G. Adhesins involved in attachment to abiotic surfaces by Gram-negative bacteria. *Microbiology Spectrum* **3,** 1–45 (2015).
6. Heiniger, R. W., Winther-Larsen, H. C., Pickles, R. J., Koomey, M. & Wolfgang, M. C. Infection of human mucosal tissue by *Pseudomonas*

aeruginosa requires sequential and mutually dependent virulence factors and a novel pilus-associated adhesin. *Cellular Microbiology* **12,** 1158–1173 (2010).

7. Chen, I. & Dubnau, D. DNA uptake during bacterial transformation. *Nature Reviews Microbiology* **2,** 241–249 (2004).

8. Harmsen, M., Yang, L., Pamp, S. J. & Tolker-Nielsen, T. An update on *Pseudomonas aeruginosa* biofilm formation, tolerance, and dispersal. *FEMS Immunology & Medical Microbiology* **59,** 253–268 (2010).

9. Mattick, J. S. Type IV Pili and Twitching Motility. *Annual Review of Microbiology* **56,** 289–314 (2002).

10. Burrows, L. L. Weapons of mass retraction. *Molecular Microbiology* **57,** 878–888 (2005).

11. Burrows, L. L. *Pseudomonas aeruginosa* Twitching Motility: Type IV Pili in Action. *Annual Review of Microbiology* **66,** 493–520 (2012).

12. Giltner, C. L., Habash, M. & Burrows, L. L. *Pseudomonas aeruginosa* Minor Pilins Are Incorporated into Type IV Pili. *Journal of Molecular Biology* **398,** 444–461 (2010).

13. Giltner, C. L., Nguyen, Y. & Burrows, L. L. Type IV pilin proteins: versatile molecular modules. *Microbiology and Molecular Biology Reviews* **76,** 740–772 (2012).

14. Nguyen, Y. *et al.* Structural and Functional Studies of the *Pseudomonas aeruginosa* Minor Pilin, PilE. *Journal of Biological Chemistry* **290,** 26856–26865 (2015).

15. Nguyen, Y. *et al. Pseudomonas aeruginosa* Minor Pilins Prime Type IVa Pilus Assembly and Promote Surface Display of the PilY1 Adhesin. *Journal of Biological Chemistry* **290,** 601–611 (2015).

16. Strom, M. S., Nunn, D. N. & Lory, S. A single bifunctional enzyme, PilD, catalyzes cleavage and N-methylation of proteins belonging to the type IV pilin family. *Proceedings of the National Academy of Sciences* **90,** 2404–2408 (1993).

17. Carter, M. Q., Chen, J. & Lory, S. The *Pseudomonas aeruginosa* pathogenicity island PAPI-1 is transferred via a novel type IV pilus. *Journal of Bacteriology* **192,** 3249–3258 (2010).

18. Chiang, P., Habash, M. & Burrows, L. L. Disparate subcellular localization patterns of *Pseudomonas aeruginosa* Type IV pilus ATPases involved in twitching motility. *Journal of Bacteriology* **187,** 829–839 (2005).

19. Whitchurch, C. B. & Mattick, J. S. Characterization of a gene, *pilU*, required for twitching motility but not phage sensitivity in *Pseudomonas aeruginosa*. *Molecular Microbiology* **13,** 1079–1091 (1994).

20. Chiang, P. *et al.* Functional role of conserved residues in the characteristic secretion NTPase motifs of the *Pseudomonas aeruginosa* type IV pilus motor proteins PilB, PilT and PilU. *Microbiology* **154,** 114–126 (2008).

21. Karuppiah, V., Hassan, D., Saleem, M. & Derrick, J. P. Structure and oligomerization of the PilC type IV pilus biogenesis protein from *Thermus*

thermophilus. *Proteins* **78,** 2049–2057 (2010).

22. Ayers, M., Howell, P. L. & Burrows, L. L. Architecture of the type II secretion and type IV pilus machineries. *Future Microbiology* **5,** 1203–1218 (2010).

23. Takhar, H. K., Kemp, K., Kim, M., Howell, P. L. & Burrows, L. L. The platform protein is essential for type IV pilus biogenesis. *The Journal of Biological Chemistry* **288,** 9721–9728 (2013).

24. Koo, J. *et al.* Functional Mapping of PilF and PilQ in the *Pseudomonas aeruginosa* Type IV Pilus System. *Biochemistry* **52,** 2914–2923 (2013).

25. Karuppiah, V. & Derrick, J. P. Structure of the PilM-PilN inner membrane type IV pilus biogenesis complex from *Thermus thermophilus*. *The Journal of Biological Chemistry* **286,** 24434–24442 (2011).

26. McCallum, M. *et al.* PilN binding modulates the structure and binding partners of the *Pseudomonas aeruginosa* Type IVa Pilus protein PilM. *Journal of Biological Chemistry* **291,** 11003–11015 (2016).

27. Tammam, S. *et al.* PilMNOPQ from the *Pseudomonas aeruginosa* type IV pilus system form a transenvelope protein interaction network that interacts with PilA. *Journal of Bacteriology* **195,** 2126–2135 (2013).

28. Sampaleanu, L. M. *et al.* Periplasmic Domains of *Pseudomonas aeruginosa* PilN and PilO Form a Stable Heterodimeric Complex. *Journal of Molecular Biology* **394,** 143–159 (2009).

29. Tammam, S. *et al.* Characterization of the PilN, PilO and PilP type IVa pilus subcomplex. *Molecular Microbiology* **82,** 1496–1514 (2011).

30. Wehbi, H. *et al.* The peptidoglycan-binding protein FimV promotes assembly of the *Pseudomonas aeruginosa* type IV pilus secretin. *Journal of Bacteriology* **193,** 540–550 (2011).

31. Demchick, P. & Koch, A. L. The Permeability of the Wall Fabric of *Escherchia coli* and *Bacillus subtilis*. *Journal of Bacteriology* **178,** 768–773 (1996).

32. Koraimann, G. Lytic transglycosylases in macromolecular transport systems of Gram-negative bacteria. *Cellular and Molecular Life Sciences* **60,** 2371–2388 (2003).

33. Scheurwater, E. M. & Burrows, L. L. Maintaining network security: how macromolecular structures cross the peptidoglycan layer. *FEMS Microbiology Letters* **318,** 1–9 (2011).

34. Herlihey, F. A., Moynihan, P. J. & Clarke, A. J. The essential protein for bacterial flagella formation FlgJ functions as a β-*N*-acetylglucosaminidase. *The Journal of Biological Chemistry* **289,** 31029–31042 (2014).

35. LeRoux, M. *et al.* Quantitative single-cell characterization of bacterial interactions reveals type VI secretion is a double-edged sword. *Proceedings of the National Academy of Sciences* **109,** 19804–19809 (2012).

36. Aschtgen, M.-S., Thomas, M. S. & Cascales, E. Anchoring the type VI secretion system to the peptidoglycan: TssL, TagL, TagP... what else?

Virulence **1,** 535–540 (2010).

37. Dower, W. J., Miller, J. F. & Ragsdale, C. W. High efficiency transformation of *E. coli* by high voltage electroporation. *Nucleic Acids Research* **16,** 6127–6145 (1988).

38. Chung, C. T., Niemela, S. L. & Miller, R. H. One-step preparation of competent *Escherichia coli*: Transformation and storage of bacterial cells in the same solution. *Proceedings of the National Academy of Sciences* **86,** 2172–2175 (1989).

39. Hoang, T. T., Karkhoff-Schweizer, R. R., Kutchma, A. J. & Schweizer, H. P. A broad-host-range Flp-FRT recombination system for site-specific excision of chromosomally-located DNA sequences: application for isolation of unmarked *Pseudomonas aeruginosa* mutants. *Gene* **212,** 77–86 (1998).

40. Shu, X., Shaner, N. C., Yarbrough, C. A., Tsien, R. Y. & Remington, S. J. Novel Chromophores and Buried Charges Control Color in mFruits. *Biochemistry* **45,** 9639–9647 (2006).

41. Cowles, K. N. *et al.* The putative Poc complex controls two distinct *Pseudomonas aeruginosa* polar motility mechanisms. *Molecular Microbiology* **90,** 923–938 (2013).

42. Asikyan, M. L., Kus, J. V. & Burrows, L. L. Novel proteins that modulate type IV pilus retraction dynamics in *Pseudomonas aeruginosa*. *Journal of Bacteriology* **190,** 7022–7034 (2008).

43. Kus, J. V. Significant differences in type IV pilin allele distribution among *Pseudomonas aeruginosa* isolates from cystic fibrosis (CF) versus non-CF patients. *Microbiology* **150,** 1315–1326 (2004).

44. Schindelin, J. *et al.* Fiji: an open-source platform for biological-image analysis. *Nature Methods* **9,** 676–682 (2012).

45. Gotoh, N., Nunomura, K. & Nishino, T. Resistance of *Pseudomonas aeruginosa* to cefsulodin: modification of penicillin-binding protein 3 and mapping of its chromosomal gene. *Journal of Antimicrobial Chemotherapy* **25,** 513–523 (1990).

46. Davis, B. M. & Waldor, M. K. Establishing polar identity in gram-negative rods. *Current Opinion in Microbiology* **16,** 752–759 (2013).

47. Hu, Z., Mukherjee, A., Pichoff, S. & Lutkenhaus, J. The MinC component of the division site selection system in *Escherichia coli* interacts with FtsZ to prevent polymerization. *Proceedings of the National Academy of Sciences* **96,** 14819–14824 (1999).

48. Burrows, L. L. A new route for polar navigation. *Molecular Microbiology* **90,** 919–922 (2013).

49. Leighton, T. L., Buensuceso, R. N. C., Howell, P. L. & Burrows, L. L. Biogenesis of *Pseudomonas aeruginosa* type IV pili and regulation of their function. *Environmental Microbiology* **17,** 4148–4163 (2015).

50. Friedrich, C., Bulyha, I. & Søgaard Andersen, L. Outside-in assembly pathway of the type IV pilus system in *Myxococcus xanthus*. *Journal of Bacteriology* **196,** 378–390 (2014).

51. Semmler, A. B. T., Whitchurch, C. B., Leech, A. J. & Mattick, J. S. Identification of a novel gene, *fimV*, involved in twitching motility in *Pseudomonas aeruginosa*. *Microbiology* **146,** 1321–1332 (2000).

52. Heidrich, C. *et al.* Involvement of *N*-acetylmuramyl-*L*-alanine amidases in cell separation and antibiotic induced autolysis of *Escherichia coli*. *Molecular Microbiology* **41,** 167–178 (2001).

53. Bernhardt, T. G. & De Boer, P. A. J. The *Escherichia coli* amidase AmiC is a periplasmic septal ring component exported via the twin-arginine transport pathway. *Molecular Microbiology* **48,** 1171–1182 (2003).

54. Peters, N. T., Dinh, T. & Bernhardt, T. G. A fail-safe mechanism in the septal ring assembly pathway generated by the sequential recruitment of cell separation amidases and their activators. *Journal of Bacteriology* **193,** 4973–4983 (2011).

55. Buist, G., Steen, A., Kok, J. & Kuipers, O. P. LysM, a widely distributed protein motif for binding to (peptido)glycans. *Molecular Microbiology* **68,** 838–847 (2008).

56. Mesnage, S. E. P. *et al.* Molecular basis for bacterial peptidoglycan recognition by LysM domains. *Nature Communications* **5,** 1–11 (2014).

57. Duncan, T. R., Yahashiri, A., Arends, S. J. R., Popham, D. L. & Weiss, D. S. Identification of SPOR domain amino acids important for septal localization, peptidoglycan binding, and a disulfide bond in the cell division protein FtsN. *Journal of Bacteriology* **195,** 5308–5315 (2013).

58. Zahrl, D. *et al.* Peptidoglycan degradation by specialized lytic transglycosylases associated with type III and type IV secretion systems. *Microbiology* **151,** 3455–3467 (2005).

59. Senf, F., Tommassen, J. & Koster, M. Polar secretion of proteins via the Xcp type II secretion system in *Pseudomonas aeruginosa*. *Microbiology* **154,** 3025–3032 (2008).

60. Michel, G. P. F. *et al.* Role of *fimV* in type II secretion system-dependent protein secretion of *Pseudomonas aeruginosa* on solid medium. *Microbiology* **157,** 1945–1954 (2011).

61. Fulcher, N. B., Holliday, P. M., Klem, E., Cann, M. J. & Wolfgang, M. C. The *Pseudomonas aeruginosa* Chp chemosensory system regulates intracellular cAMP levels by modulating adenylate cyclase activity. *Molecular Microbiology* **76,** 889–904 (2010).

62. Siewering, K. *et al.* Peptidoglycan-binding protein TsaP functions in surface assembly of type IV pili. *Proceedings of the National Academy of Sciences* **111,** E953–E961 (2014).

63. Braun, V. Energy-coupled transport and signal transduction through the Gram-negative outer membrane via TonB-ExbB-ExbD-dependent receptor proteins. *FEMS Microbiology Reviews* **16,** 295–307 (1995).

64. Kaserer, W. A. *et al.* Insight from TonB hybrid proteins into the mechanism of iron transport through the outer membrane. *Journal of Bacteriology* **190,** 4001–4016 (2008).

65. de Pedro, M. A., Quintela, J. C., Holtje, J.-V. & Schwarz, H. Murein segregation in *Escherichia coli*. *Journal of Bacteriology* **179,** 2823–2834 (1997).

66. Helm, R. A., Barnhart, M. M. & Seifert, H. S. *pilQ* Missense Mutations Have Diverse Effects on PilQ Multimer Formation, Piliation, and Pilus Function in *Neisseria gonorrhoeae*. *Journal of Bacteriology* **189,** 3198–3207 (2007).

67. Gray, A. N. *et al.* Coordination of peptidoglycan synthesis and outer membrane constriction during *Escherichia coli* cell division. *eLIFE* 1–29 (2015). doi:10.7554/eLife.07118.001

68. Nudleman, E., Wall, D. & Kaiser, D. Cell-to-cell Transfer of Bacterial Outer Membrane Lipoproteins. *Science* **309,** 125–127 (2005).

69. Kilmury, S. L. N. & Burrows, L. L. Type IV pilins regulate their own expression via direct intramembrane interactions with the sensor kinase PilS. *Proceedings of the National Academy of Sciences* **113,** 6017–6022 (2016).

70. Goldberg, J. B. in *Pseudomonas* 141–175 (Springer Netherlands, 2010). doi:10.1007/978-90-481-3909-5_5

71. Wei, H.-L. & Collmer, A. Multiple lessons from the multiple functions of a regulator of type III secretion system assembly in the plant pathogen *Pseudomonas syringae*. *Molecular Microbiology* **85,** 195–200 (2012).

72. Simon, R., Priefer, U. & Puhler, A. A Broad Host Range Mobilization System for *in vivo* Genetic Engineering: Transposon Mutagenesis in Gram Negative Bacteria. *Nature Biotechnology* **1,** 784–791 (1983).

73. Ayers, M. *et al.* PilM/N/O/P Proteins Form an Inner Membrane Complex That Affects the Stability of the *Pseudomonas aeruginosa* Type IV Pilus Secretin. *Journal of Molecular Biology* **394,** 128–142 (2009).

74. Kus, J. V. *et al.* Modification of *Pseudomonas aeruginosa* Pa5196 Type IV Pilins at Multiple Sites with D-Ara*f* by a Novel GT-C Family Arabinosyltransferase, TfpW. *Journal of Bacteriology* **190,** 7464–7478 (2008).

75. Buensuceso, R. N. C. *et al.* The conserved TPR-containing C-terminal domain of *Pseudomonas aeruginosa* FimV is required for its cAMP-dependent and independent functions. *Journal of Bacteriology* **198,** 2263–2274 (2016).

Section 7 – APPENDIX

Table 1. Bacterial strains and vectors

Strain	Description	Source
E. coli		
DH5α	F-, φ80lacZ, M15, Δ(*lacZYA-argF*), U169, *recA1, endA1, hsdR17(rk-,mk+), phoAsupE44, thi-1, gyrA96, relA1*, λ-	Invitrogen
SM10	*thi-1, thr, leu, tonA, lacy, supE, recA*, RP4-2-Tcr::Mu, Kmr; mobilizes plasmids into *P. aeruginosa* via conjugation	[72]
P. aeruginosa		
PAK	Wild-type	J. Boyd
ΔpilM	Deletion of *pilM*	[73]
pilP::FRT	FRT scar at position 86 within *pilP*	[73]
pilQ::FRT	FRT scar at position 571 within *pilQ*	[24]
pilA::FRT	FRT scar at SphI site within *pilA*	[74]
ΔpilF	Deletion of *pilF*	This study
ΔminC	Deletion of *minC*	This study
mCherry-PilO	Insertion of *mCherry* at the 5' end of *pilO*	This study
ΔpocA	Deletion of *pocA*	[41]
ΔfimV	Deletion of *fimV*	[75]
*fimV*ΔLysM	*fimV* containing deletion of LysM domain	[30]
mCherry-PilO/*ΔpilM*	Insertion of *mCherry* at the 5' end of *pilO* with deletion of *pilM*	This study
mCherry-PilO/*pilP*::FRT	Insertion of *mCherry* at	This study

	the 5' end of *pilO* with FRT scar at position 86 within *pilP*	
mCherry-PilO/*pilQ*::FRT	Insertion of *mCherry* at the 5' end of *pilO* with FRT scar at position 571 within *pilQ*	This study
mCherry-PilO/*ΔpilF*	Insertion of *mCherry* at the 5' end of *pilO* with deletion of *pilF*	This study
mCherry-PilO/*ΔminC*	Insertion of *mCherry* at the 5' end of *pilO* with deletion of *minC*	This study
mCherry-PilO/*ΔpocA*	Insertion of *mCherry* at the 5' end of *pilO* with deletion of *pocA*	This study
mCherry-PilO/*ΔfimV*	Insertion of *mCherry* at the 5' end of *pilO* with deletion of *fimV*	This study
mCherry-PilO/*fimV*ΔLysM	Insertion of *mCherry* at the 5' end of *pilO* with *fimV* containing deletion of LysM domain	This study
Vector	**Description**	**Source**
pEX18Gm	Suicide vector used for gene replacement, Gm	[39]
pEX18Ap	Suicide vector used for gene replacement, Ap	[39]
pBADGr	Arabinose inducible protein expression vector	[42]
pFLP2	Suicide vector containing Flp recombinase	[39]
pEX18Gm::*mCherry-pilO*	Suicide vector containing *mCherry-pilO*, cloned using EcoRI/HindIII	This study
pEX18Gm::*ΔpilF*	Suicide vector containing *pilF* deletion, cloned using BamHI/HindIII	This study
pEX18Gm::*ΔminC*	Suicide vector containing *minC* deletion, cloned using BamHI/HindIII	This study

pEX18Gm::*ΔpocA*	Suicide vector containing *pocA* deletion, cloned using EcoRI/XbaI	This study
pEX18Ap::*pilQ*::FRTGmFRT	Suicide vector containing PAK *pilQ* disrupted with FRT-flanked Gm cassette at position 571	[24] and this study
pBADGr::*pilQ-mCherry*	*pilQ-mCherry* complementation construct, cloned using EcoRI/HindIII	This study
pBADGr::*pilF*	*pilF* complementation construct, cloned using SphI/HindIII	This study
pBADGr::*pilQ*	*pilQ* complementation construct, cloned using EcoRI/HindIII	This study
pBADGr::*pilQΔAmiN*	*pilQΔAmiN* complementation construct, cloned using EcoRI/HindIII	This study
pBADGr::*pocA*	*pocA* complementation construct, cloned using EcoRI/HindIII	This study
pBADGr::*fimV-yfp*	*fimV-yfp* complementation construct, cloned using KpnI/XbaI	This study

Table 2. Oligonucleotide sequences

| Name	Oligonucleotide sequence
PilF-Fwd	5'ACGCCTTGCAAGATCAACCTGATTCCG3'
PilF-Rev	5'TCGAACGCGCCGTTTTCCAGCTGACGC3'
PilF mid-Rev	5'GGCCGGTTTCTTCATTTGCAGCG3'
PilF Clone-Fwd	5'TCATGCATGCATGACTGTACGCGCCGCGCTGG3'

PilF Clone-Rev	5'TCATAAGCTTTCATTTTTCCGCCTGGAATTCCTG3'
MinC Fwd	5'GGATACGGCAACTGCACCACCAGCCAG3'
MinC Rev	5'GACGACGTTGACGAAGTCGTACACCAC3'
MinC mid-Rev	5'CGTGGCGGCGACAGACCTCGAGGA3'
PilN 3'-Fwd	5'GCCAACGTGTTCCAACTG3'
PilO Rev	5'CCACGCTGATCTGGATCG3'
PocA Fwd	5'GAATTCGGGGATATGCCACGTGTGGGA3'
PocA Rev	5'AAGCTTTGCGGCGGAATTTCACGCTTTGC3'
PocA Mid-Rev	5'GAGGATCTCTCCCAGCGG3'
PocA Clone-Fwd	5'TCATGAATTCGTGTGGGAACTGGTTCAAGCCGG3'
PocA Clone-Rev	5'TCATAAGCTTTCACGCTTTGCCTTCCTCGACGTAG3'
PilQ Clone-Fwd	5'AGAATTCCAACAGCAGTCTGTACAA3'
PilQ Clone-Rev	5'TCATAAGCTTTCAGCGACCGATTGCGATGGCCTG3'
PilQ 910-Fwd	5'CGACCTGAATCTGGTGGC3'
PilQ FRT-Chk Fwd	5'TTGATCATCAACCTGACCGCGCTGTCG3'
PilQ FRT-Chk Rev	5'TCATCGGCTTGATGCTGACGGTCAGG3'
pBAD mcs-Fwd	5'AAGTGTCTATAATCACGGCAGA3'

|	
pBAD mcs-Rev	5'TCACTTCTGAGTTCGGCATGG3'
mCherry Rev	5'TCATGCATGCGCTTCCGCCGCTCTTGTACAGCTCGTCCATGCCGC3'
PilQ 5' Rev	5'TCATTCTAGAGTCCGCGGCGAGCAATGCCGGCGC3'
PilQ N0 Fwd	5'TCATTCTAGAGGCGAGAAACTGTCGCTGAACTTC3'
FimV Clone Fwd	5'GCGGGTACCATGGTTCGGCTTCG3'
FimV Clone Rev	5'GCGTCTAGAGGCCAGGCGCTCCA3'

Table 3. Antisera and dilution factors

Antisera	Dilution
α-PilM	1:1000
α-PilO	1:3000
α-PilP	1:5000
α-PilQ	1:3000
α-PilF	1:3000
α-FimV (periplasmic epitope)	1:3000
α-mCherry	1:1000
α-GFP	1:5000
Goat α-Rabbit-AP conjugate	1:3000
Goat α-Mouse-AP conjugate	1:3000

Supplementary Figure 1.
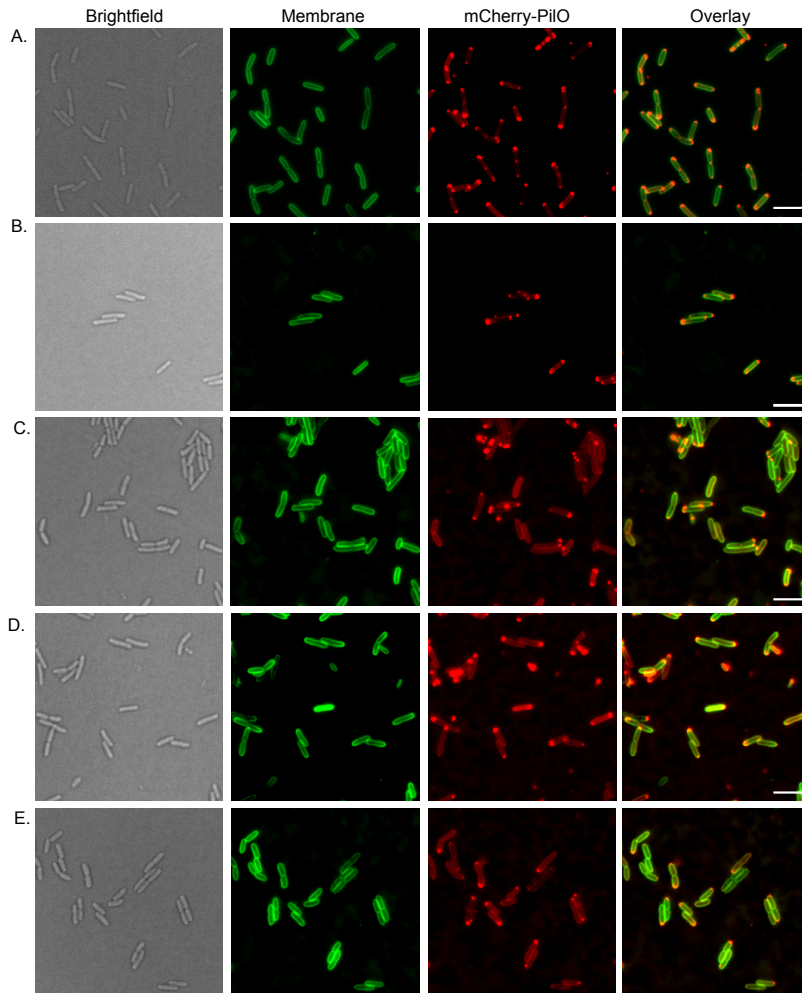
Supplementary Figure 1. PilQ-mCherry is partly delocalized in untreated *poc* and *fimV* mutants. A) When PilQ-mCherry is introduced into *pilQ* mutant cells the fusion localizes to the poles and septum as well as regularly spaced intervals when treated with 40 µg/ml cefsulodin. B) In the absence of the pilotin, PilF, inner membrane situated PilQ-mCherry monomers localize to the poles and regularly spaced intervals in cefsulodin treated cells. C) In the absence of FimV, PilQ-mCherry is delocalized to an extent because peripheral fluorescence in prominent, although polar foci are present. D) When FimV is missing its PG-binding domain, the LysM domain, PilQ-mCherry is delocalized in the same fashion as a *fimV* mutant. E) In the absence of PocA, PilQ-mCherry is delocalized to the same extent as the *fimV* mutants. Scale Bar = 3 µm. The PilQ-mCherry construct was expressed using the pBADGr expression vector in *P. aeruginosa* cells. Cell membranes are stained using FM1-43FX dye (in 10 µg/ml dye solution). Cells were stab-inoculated into 1% LBA in chambered glass coverslips, incubated at 37°C and imaged using the 63x oil immersion objective on an EVOS-FL digital imaging system. Images were processed using Fiji.

Supplementary Figure 2
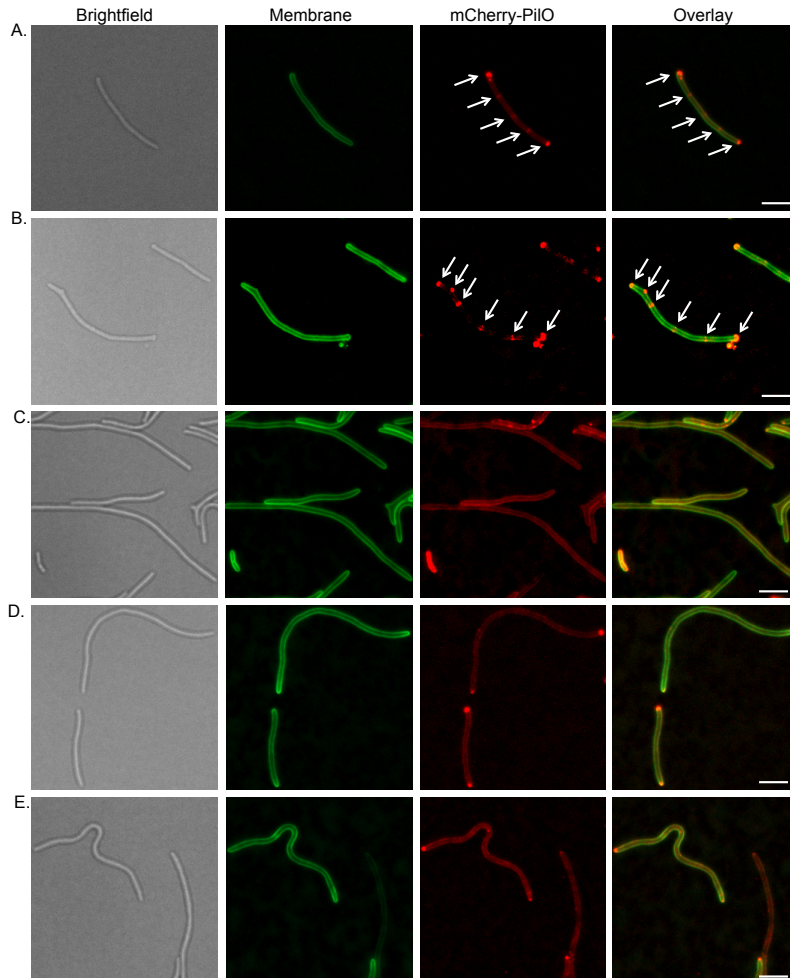
Supplementary Figure 2. PilQ-mCherry delocalization is evident in filamented cells. A) When PilQ-mCherry is introduced into *pilQ* mutant cells the fusion localizes to the poles as well as regularly spaced intervals (arrows) when treated with 40 µg/ml cefsulodin. B) In the absence of the pilotin, PilF, inner membrane situated PilQ-mCherry monomers localize to the poles and regularly spaced intervals (arrows) in cefsulodin treated cells. C) In the absence of FimV, PilQ-mCherry is mislocalized in treated cells. D) When FimV is missing its PG-binding domain, the LysM domain, PilQ-mCherry is delocalized. E) In the absence of PocA, PilQ-mCherry is delocalized. Scale Bar = 3 µm. The PilQ-mCherry construct was expressed using the pBADGr expression vector in *P.* aeruginosa cells. Cell membranes are stained using FM1-43FX dye (in 10 µg/ml dye solution). Cells were stab-inoculated into 1% LBA in chambered glass coverslips, incubated at 37°C and imaged using the 63x oil immersion objective on an EVOS-FL digital imaging system. Images were processed using Fiji.